



UNIVERSIDADE ESTADUAL DE MARINGÁ
Departamento de Farmácia
Programa de Pós-Graduação em Ciências Farmacêuticas



**APLICAÇÃO DA BIOTECNOLOGIA NA OBTENÇÃO DE
PRODUTOS FARMACÊUTICOS E ALIMENTÍCIOS
INOVADORES DE ORIGEM ANIMAL E VEGETAL**

JULIANA HARUMI MIYOSHI

Maringá

2024

JULIANA HARUMI MIYOSHI

**Aplicação da biotecnologia na obtenção de produtos
farmacêuticos e alimentícios inovadores de origem
animal e vegetal**

Tese apresentada ao Programa de Pós-Graduação em Ciências Farmacêuticas (Área de Concentração: Produtos Naturais e Sintéticos Biologicamente Ativos), da Universidade Estadual de Maringá, como parte dos requisitos para obtenção do Título de Doutora em Ciências Farmacêuticas.

Orientadora: Prof^a. Dr^a. Graciete Matioli
Co-orientadora: Prof^a. Dr^a. Gislaine Franco de Moura Costa

Maringá

2024

Dados Internacionais de Catalogação-na-Publicação (CIP)
(Biblioteca Central - UEM, Maringá - PR, Brasil)

M685a	<p>Miyoshi, Juliana Harumi Aplicação da biotecnologia na obtenção de produtos farmacêuticos e alimentícios inovadores de origem animal e vegetal / Juliana Harumi Miyoshi. – Maringá, PR, 2024. 70 f. : il. color., figs., tabs.</p> <p>Orientadora: Profa. Dra. Gracielle Matioli. Coorientadora: Profa. Dra. Gislaine Franco de Moura Costa. Tese (Doutorado) - Universidade Estadual de Maringá, Centro de Ciências da Saúde, Departamento de Farmácia, Programa de Pós-Graduação em Ciências Farmacêuticas, 2024.</p> <p>1. Biotecnologia enzimática - Tripsina. 2. Aromas cárneos - Quimotripsina. 3. Óleos essenciais - Peptídeos bioativos. 4. Ciclodextrina. 5. Produtos farmacêuticos e alimentícios. I. Matioli, Gracielle, orient. II. Costa, Gislaine Franco de Moura, coorient. III. Universidade Estadual de Maringá. Centro de Ciências da Saúde. Departamento de Farmácia. Programa de Pós-Graduação em Ciências Farmacêuticas. IV. Título.</p>
	CDD 23.ed. 615.3 Ademir Henrique dos Santos - CRB-9/1065

JULIANA HARUMI MIYOSHI

APLICAÇÃO DA BIOTECNOLOGIA NA OBTENÇÃO DE PRODUTOS FARMACÊUTICOS E ALIMENTÍCIOS INOVADORES DE ORIGEM ANIMAL E VEGETAL

153^a Tese apresentada ao Programa de Pós-Graduação em Ciências Farmacêuticas da Universidade Estadual de Maringá como requisito para obtenção do título de Doutor em Ciências Farmacêuticas.

Aprovada em 05 de março de 2024

BANCA EXAMINADORA

Gracielle Matoli

Dra. Gracielle Matoli

Universidade Estadual de Maringá

 Documento assinado digitalmente
EDMARDO CESAR MEURER
Data: 11/03/2024 10:14:11 -0300
Verifique em <https://validacao.gouv.br>

Dra. Camila Sampaio Mangolin
Universidade Federal da Paraíba

 Documento assinado digitalmente
EDMARDO CESAR MEURER
Data: 11/03/2024 10:14:11 -0300
Verifique em <https://validacao.gouv.br>

Dr. Eduardo César Meurer
Universidade Federal do Paraná

 Documento assinado digitalmente
FRANCIELLE SATO
Data: 11/03/2024 10:14:11 -0300
Verifique em <https://validacao.gouv.br>

Dra. Francielle Sato
Universidade Estadual de Maringá

 Documento assinado digitalmente
SUELLEN PEREIRA RUIZ HERRIG
Data: 10/03/2024 22:51:46 -0300
Verifique em <https://validacao.gouv.br>

Dra. Suelen Pereira Ruiz Herrig
Universidade Paranaense

AUTORIZO A REPRODUÇÃO E A DIVULGAÇÃO PARCIAL (RESUMO) DESTE TRABALHO, POR QUALQUER MEIO CONVENCIONAL OU ELETRÔNICO, PARA FINS DE PESQUISA OU ESTUDO E PESQUISA, DESDE QUE CITADA A FONTE.

Dedico

À Deus. Dedico, também, aos meus pais Ricardo e Dalzira que sempre me apoiaram, e às minhas irmãs Cláudia e Ana Carolina. Por fim, dedico à minha orientadora, Professora Doutora Graciette Matioli, e à Professora Doutora Gislaine Franco de Moura Costa, minha co-orientadora.

AGRADECIMENTOS

Primeiramente, agradeço à Deus, criador do Universo, que permitiu que este momento se realizasse, trazendo alegria aos meus pais e a todos que contribuíram para a realização deste trabalho. Agradeço aos meus pais, Ricardo e Dalzira, pela oportunidade que me deram de cursar o ensino superior, o mestrado e todo o apoio deles durante toda a minha vida, sem medir esforços para que eu pudesse concluir mais uma etapa na minha vida, o doutorado. Às minhas irmãs, Cláudia e Ana Carolina, por estarem sempre ao meu lado, assim como toda minha família.

À minha orientadora, Professora Doutora Graciette Matioli, pela oportunidade de atuar no Laboratório de Biotecnologia Enzimática (LaBE) durante minha graduação, mestrado e doutorado, pelo conhecimento adquirido, pela sua orientação e amizade, pelo apoio e confiança. À minha co-orientadora, Professora Doutora Gislaine Franco de Moura Costa, pelo apoio e confiança. A toda a equipe do LaBE, agradeço a amizade e companheirismo durante essa jornada. Aos meus amigos agradeço por todo o apoio, amor, amizade, companheirismo e por me ajudar em todo o processo, vocês sempre farão parte da minha vida. Agradeço aos meus pequenos, Nickolas e Amora por serem meus companheirinhos e meu suporte emocional nesses anos. Aos professores que colaboraram com os resultados do trabalho, cedendo seu tempo e laboratório para que fossem realizadas as análises. À empresa BRF e ao supervisor José Maluf por aceitar esse desafio e por todo suporte oferecido para o desenvolvimento desse estudo.

Ao Programa de Pós-graduação em Ciências Farmacêuticas (PCF) e à Universidade Estadual de Maringá (UEM) pela oportunidade de me fazer doutora. Agradeço à Francisca Helena M. de Carvalho pela sua dedicação na secretaria do PCF, nos dando atenção e assistência em diversas situações. Por fim, agradeço ao CNPq pela concessão das bolsas de estudo que possibilitaram a minha dedicação integral a esta pesquisa. E, mais uma vez, ao CNPq, à Fundação Araucária, à CAPES, Central Analítica Multusuário de Medianeira e ao FINEP pelo apoio financeiro que possibilitou a infraestrutura utilizada para a execução da pesquisa.

A todos que, direta ou indiretamente, fizeram parte da minha formação, o meu muito obrigada.

“O homem não teria alcançado o possível se, repetidas vezes, não tivesse tentado o impossível.”

(Max Weber)

APRESENTAÇÃO

Esta pesquisa foi desenvolvida com o apoio de uma equipe multidisciplinar por meio de parcerias estabelecidas entre o Laboratório de Biotecnologia Enzimática (LaBE) do Departamento de Farmácia da Universidade Estadual de Maringá (DFA-UEM), empresa BR Foods S.A., Complexo de Centrais de Apoio a Pesquisa (COMCAP-UEM), Laboratório de Espectrometria de Massas - FEM (UFPR), Central Analítica Multiusuário de Medianeira (UTFPR).

A presente tese de doutorado está apresentada na forma de dois artigos científicos:

I - AUTORES: Juliana Harumi Miyoshi, Thamara Thaiane da Silva Crozatti, Laira Machado Brandão Toller, Marco Aurélio Schuler Oliveira, Jose Uebi Maluf, Tieles Carina Oliveira Delani, Giovanni Cesar Teles, Eduardo Cesar Meurer e Graciette Matioli.

TÍTULO: HIDRÓLISE ENZIMÁTICA DE AROMAS CÁRNEOS PARA OBTENÇÃO DE COLÁGENO E PEPTÍDEOS BIOATIVOS

II - AUTORES: Juliana Harumi Miyoshi, Thamara Thaiane da Silva Crozatti, Júlia Rosa de Brito, Henrique dos Santos, Ana Cláudia Nogueira Mulati, Leandro Herculano da Silva, Francielle Sato, Juliana Cristina Castro, Gislaine Franco de Moura Costa e Graciette Matioli

TÍTULO: COMPLEXAÇÃO DE ÓLEOS ESSENCIAIS COM BETA-CICLODEXTRINA: CARACTERIZAÇÃO DOS COMPLEXOS, DETERMINAÇÃO DAS ATIVIDADES ANTIMICROBIANA, ANTIOXIDANTE E APLICAÇÃO

REVISTA: Food Hydrocolloids

Artigo submetido (Qualis A1).

MIYOSHI, J. H. 2024. Aplicação da biotecnologia na obtenção de produtos farmacêuticos e alimentícios inovadores de origem animal e vegetal. Tese de doutorado. Programa de Pós-graduação em Ciências Farmacêuticas, Universidade Estadual de Maringá, p. 69.

RESUMO GERAL

A transformação ou invenção de um novo produto, ideia ou serviço está ligada diretamente ao processo criativo e inovador, além de facilitar e melhorar a qualidade de vida da sociedade. Sendo assim, o Programa de Doutorado Acadêmico em Inovação (DAI), na qual é uma iniciativa do Conselho Nacional de Desenvolvimento Científico e Tecnológico (CNPq) surgiu para que os Programas de Pós-Graduação possam fomentar projetos em parceria com empresas no desenvolvimento e/ou criação de produtos e tecnologias. Considerando o exposto acima, esta tese teve como foco a utilização da biotecnologia na obtenção de produtos farmacêuticos e alimentícios inovadores, apresentada na forma de dois artigos científicos.

ARTIGO I - HIDRÓLISE ENZIMÁTICA DE AROMAS CÁRNEOS PARA EXTRAÇÃO DE COLÁGENO E OBTENÇÃO PEPTÍDEOS BIOATIVOS

INTRODUÇÃO. A indústria alimentícia gera grande quantidade de resíduos orgânicos, e quando não descartados corretamente são considerados uma fonte importante de contaminação ambiental. A reciclagem apresenta-se como melhor via de destinação, uma vez que os resíduos citados podem transformar-se em produtos comerciais com maior valor agregado, incluindo os comestíveis, semiprocessados ou destinados a outras aplicações. Os aromas de frango e carne são produtos ricos em proteínas, carboidratos e lipídeos, que agregarem sabor e odor natural ao alimento. Uma proteína que está presente nos aromas é o colágeno, o qual pode ser obtido e hidrolisado com a utilização de enzimas. A hidrólise enzimática também pode ser uma possibilidade para obtenção de peptídeos bioativos e solucionar a procura por processos sustentáveis para gestão de resíduos provenientes das indústrias de alimentos.

OBJETIVOS. Considerando a importância da gestão de subprodutos, a necessidade de melhorar as características funcionais de produtos industrializados e aumentar o seu valor, a presente pesquisa teve como objetivo a obtenção do colágeno de aromas cárneos com a utilização de enzimas e a avaliação dos peptídeos bioativos resultantes do processo de hidrólise.

MATERIAL E MÉTODOS. Os aromas de frango e de carne foram fornecidos pela empresa BRF Ingredients (Brasil). Foi realizada a hidrólise enzimática dos aromas utilizando a enzimas quimotripsina em diferentes condições de temperatura, concentração e tempo de reação e em seguida adicionados a enzima tripsina. Foi determinado o teor de proteína bruta, o grau de hidrólise e feito a eletroforese em gel dos aromas e seus respectivos hidrolisados. Por fim, foi determinado o teor de colágeno em todas as amostras e realizado a identificação dos peptídeos bioativos por espectrometria de massas sequencial.

RESULTADOS E DISCUSSÃO. A quantidade de proteína bruta foi acima de 69% para o aroma de frango e seus respectivos hidrolisados, porém, para o aroma de carne, esse valor foi inferior a 20%. Na eletroforese foi confirmada a hidrólise dos materiais, bem como o alto grau de hidrólise do aroma de carne e seus respectivos hidrolisados. O teor de colágeno para o aroma de frango foi de aproximadamente 23%, enquanto seus hidrolisados foram superiores a 27%. Para o aroma de carne o teor de colágeno foi aproximadamente 4% e seus hidrolisados não apresentaram quantidades significativas de colágeno. Na temperatura de 30 °C, 25% de enzima

e 6 h de ensaio, o aroma de frango forneceu maior quantidade de peptídeos bioativos, na qual a prevalência de atividade foi o inibidor da dipeptidil peptidase IV, utilizado em medicamentos anti-hiperglicêmicos.

CONCLUSÕES. O processo de hidrólise enzimática dos aromas de frango e carne utilizando as enzimas quimotripsina e tripsina para a obtenção de colágeno e peptídeos bioativos foi satisfatória, especialmente para o aroma de frango. Os peptídeos bioativos foram identificados com metodologia inovadora por LC-MS e apresentaram atividades anti-hipertensiva e antidiabéticas. Portanto, com esta pesquisa foi possível a utilização de processos biotecnológicos para melhorar as características dos aromas cárneos, bem como agregar valor ao produto, sendo uma alternativa para as indústrias farmacêuticas e alimentícia.

Palavras-chave: biotecnologia enzimática, quimotripsina, tripsina, subprodutos cárneos, peptídeos bioativos.

ARTIGO II - COMPLEXAÇÃO DE ÓLEOS ESSENCIAIS COM BETA-CICLODEXTRINA: CARACTERIZAÇÃO DOS COMPLEXOS, DETERMINAÇÃO DAS ATIVIDADES ANTIMICROBIANA, ANTIOXIDANTE E APLICAÇÃO

INTRODUÇÃO. Os óleos essenciais são produtos do metabolismo secundário das plantas aromáticas e possuem diversas propriedades bioativas. O coentro e o orégano são plantas aromáticas com potencial biológico, porém a utilização desses óleos é limitada devido sua instabilidade e insolubilidade em água e, uma alternativa para melhorar essas características é a encapsulação utilizando agentes complexantes como as ciclodextrinas. As ciclodextrinas são moléculas em formato de cone truncado com cavidade hidrofóbica, sendo excelente hospedeira para as moléculas hidrofóbicas presentes nos óleos essenciais.

OBJETIVOS. A pesquisa teve como objetivo encapsular os óleos essenciais de coentro e orégano com a beta-ciclodextrina, caracterizar o óleo essencial e os complexos de inclusão formados pelas metodologias de amassamento e co-precipitação, avaliar a atividade antimicrobiana e antioxidante dos óleos essenciais livres e complexados e incorporar em um produto alimentício.

MATERIAL E MÉTODOS. Foram utilizados os óleos essenciais de coentro (*Coriandrum sativum L.*) e orégano (*Origanum vulgare*), os quais foram caracterizados por cromatografia gasosa acoplada ao massas. Os complexos de inclusão foram feitos utilizando a beta-ciclodextrina como agente complexante pelas metodologias de amassamento e co-precipitação. Ensaios de eficiência da complexação foram executados e a caracterização dos complexos foi realizada pelas técnicas de espectroscopia de infravermelho por transformada de Fourier acoplado com acessório de refletância total atenuada (FTIR-ATR), Micro-Raman, calorimetria diferencial de varredura e termogravimetria. A atividade antioxidante foi realizada pelas metodologias de determinação dos compostos fenólicos e das atividades sequestrantes de radicais livres pelos métodos de ABTS⁺ e DPPH. Os métodos de microdiluição em caldo e difusão em ágar foram utilizados para determinar a atividade antimicrobiana dos óleos essenciais e seus complexos de inclusão. Por fim, o óleo essencial que apresentou melhores resultados foi incorporado na manteiga e avaliado a estabilidade oxidativa pelo método Rancimat.

RESULTADOS E DISCUSSÃO. Os compostos majoritários presentes nos óleos essenciais de coentro e orégano foram o linalol e carvacrol, respectivamente, em quantidades superiores a 62% da composição total. A eficiência da complexação foi melhor para os complexos formados pela metodologia de co-precipitação. Na caracterização dos complexos de inclusão por FTIR-ATR e Micro-Raman foi possível observar diversos deslocamentos no espectro, evidenciando a formação dos complexos de inclusão por ambas as metodologias. Nas análises térmicas foi verificado o desaparecimento do pico característico da evaporação da água presente na cavidade da beta-ciclodextrina, sugerindo que os óleos essenciais deslocaram a água e se inseriram nesta cavidade. Os óleos essenciais apresentaram atividade antimicrobiana e os compostos envolvidos nesta atividade foram linalol, timol e carvacrol. A melhor resposta foi obtida com a metodologia de difusão em ágar, no qual os complexos de inclusão apresentaram melhor atividade. Considerando que somente o óleo essencial de orégano apresentou atividade antioxidante, a estabilidade frente às altas temperaturas foi realizada com este óleo, na qual os complexos apresentaram grande estabilidade. A incorporação do óleo essencial de orégano e seus complexos na manteiga resultou numa melhor estabilidade oxidativa em relação à manteiga sem a adição dos mesmos.

CONCLUSÕES. A formação dos complexos de inclusão pelas metodologias de amassamento e co-precipitação foi confirmada pelos métodos físico-químicos e o processo de complexação apresentou resultados positivos para as atividades antimicrobianas e antioxidantes. A incorporação do óleo essencial de orégano e seus complexos na manteiga foi promissora, garantiu proteção antimicrobiana e estabilidade oxidativa ao produto.

Palavras-chave: *Coriandrum sativum*, *Origanum vulgare*, ciclodextrina, complexo de inclusão, proteção oxidativa.

MIYOSHI, J. H. 2024. Application of biotechnology to obtain innovative pharmaceutical and food products of animal and plant origin. Doctoral thesis. Post-graduation Program in Pharmaceutical Sciences, State University of Maringá, p. 69.

GENERAL ABSTRACT

The transformation or invention of a new product, idea or service is directly linked to the creative and innovative process, in addition to facilitating and improving society's quality of life. Therefore, the Academic Doctorate Program in Innovation (DAI), which is an initiative of the National Council for Scientific and Technological Development (CNPq) emerged so that Postgraduate Programs can promote projects in partnership with companies in development and/or creation of products and technologies. Considering the above, this thesis focused on the use of biotechnology to obtain innovative pharmaceutical and food products, presented in the form of two scientific articles.

ARTICLE I - ENZYMATIC HYDROLYSIS OF MEAT FLAVORS TO OBTAIN COLLAGEN AND BIOACTIVE PEPTIDES

INTRODUCTION. The food industry generates a large amount of organic waste, and when not disposed of correctly, it is considered an important source of environmental contamination. Recycling is the best method of disposal, since the aforementioned waste can be transformed into commercial products with greater added value, including edible, semi-processed or intended for other applications. Chicken and meat flavors are products rich in proteins, carbohydrates and lipids, which add flavor and natural odor to the food. A protein that is present in aromas is collagen, which can be obtained and hydrolyzed using enzymes. Enzymatic hydrolysis can also be a possibility for obtaining bioactive peptides and solving the search for sustainable processes for waste management from the food industry.

AIMS. Considering the importance of waste management, the need to improve the functional characteristics of industrialized products and increase their value, the present research aimed to obtain collagen from meat aromas using enzymes and evaluate the bioactive peptides resulting from the hydrolysis process.

MATERIAL AND METHODS. The chicken and meat aromas were supplied by the company BRF Ingredients (Brazil). Enzymatic hydrolysis of the aromas was carried out using chymotrypsin enzymes under different conditions of temperature, concentration and reaction time and then added the trypsin enzyme. The crude protein content and the degree of hydrolysis were determined and gel electrophoresis of the aromas and their respective hydrolysates was performed. Finally, the collagen content in all samples was determined and bioactive peptides were identified by sequential mass spectrometry.

RESULTS AND DISCUSSION. The amount of crude protein was above 69% for the chicken flavor and its respective hydrolysates, however, for the meat flavor, this value was less than 20%. In electrophoresis, the hydrolysis of the materials was confirmed, as well as the high degree of hydrolysis of the meat aroma and its respective hydrolysates. The collagen content for the chicken flavor was approximately 23%, while its hydrolysates were greater than 27%. For the meat flavor, the collagen content was approximately 4% and its hydrolysates did not present significant amounts of collagen. At a temperature of 30 °C, 25% enzyme and 6 h of assay, the chicken flavor provided a greater amount of bioactive peptides, in which the prevalence of activity was the dipeptidyl peptidase IV inhibitor, used in antihyperglycemic medications.

CONCLUSIONS. The process of enzymatic hydrolysis of chicken and meat flavors using the enzymes chymotrypsin and trypsin to obtain collagen and bioactive peptides was satisfactory, especially for the chicken flavor. The bioactive peptides were identified using innovative LC-MS methodology and showed antihypertensive and antidiabetic activities. Therefore, with this research it was possible to use biotechnological processes to improve the characteristics of meat flavors, as well as adding value to the product, being an alternative for the pharmaceutical and food industries.

Keywords: enzyme biotechnology, chymotrypsin, trypsin, meat by-products, bioactive peptides.

ARTICLE II - COMPLEXATION OF ESSENTIAL OILS WITH BETA-CYCLODEXTRIN: CHARACTERIZATION OF COMPLEXES, DETERMINATION OF ANTIMICROBIAL, ANTIOXIDANT ACTIVITIES AND APPLICATION

INTRODUCTION. Essential oils are products of the secondary metabolism of aromatic plants and have several bioactive properties. Coriander and oregano are aromatic plants with biological potential, however the use of these oils is limited due to their instability and insolubility in water, and an alternative to improving these characteristics is encapsulation using complexing agents such as cyclodextrins. Cyclodextrins are truncated cone-shaped molecules with a hydrophobic cavity, making them an excellent host for the hydrophobic molecules present in essential oils.

AIMS. Considering the applicability of essential oils, their instability and low solubility, this research aimed to encapsulate coriander and oregano essential oils with beta-cyclodextrin, characterize the essential oil and the inclusion complexes formed by kneading and co-precipitation, evaluate the antimicrobial and antioxidant activity of free and complexed essential oils and incorporate them into a food product.

MATERIAL AND METHODS. Coriander (*Coriandrum sativum* L.) and oregano (*Origanum vulgare*) essential oils were used, which were characterized by mass-coupled gas chromatography. The inclusion complexes were made using beta-cyclodextrin as a complexing agent by kneading and co-precipitation methodologies. Complexation efficiency tests were performed and the characterization of the complexes was carried out using Fourier transform infrared (FTIR) spectrometer accessorized with attenuated total reflectance (FTIR-ATR), Micro-Raman, differential scanning calorimetry and thermogravimetry. The antioxidant activity was carried out using the methodologies for determining phenolic compounds and the free radical scavenging activities using the ABTS^{•+} and DPPH methods. Broth microdilution and agar diffusion methods were used to determine the antimicrobial activity of essential oils and their inclusion complexes. Finally, the essential oil that showed the best results was incorporated into the butter and its oxidative stability was evaluated using the Rancimat method.

RESULTS AND DISCUSSION. The main compounds present in coriander and oregano essential oils were linalool and carvacrol, respectively, in amounts greater than 62% of the total composition. The complexation efficiency was better for the complexes formed by the co-precipitation methodology. When characterizing the inclusion complexes by FTIR-ATR and Micro-Raman, it was possible to observe several shifts in the spectrum, demonstrating the formation of inclusion complexes by both methodologies. In thermal analyses, the characteristic

peak of the evaporation of water present in the beta-cyclodextrin cavity disappeared, suggesting that the essential oils displaced the water and were inserted into this cavity. Essential oils showed antimicrobial activity and the compounds involved in this activity were linalool, thymol and carvacrol. The best response was obtained with the agar diffusion methodology, in which the inclusion complexes showed better activity. Considering that only oregano essential oil showed antioxidant activity, stability against high temperatures was achieved with this oil, in which the complexes showed great stability. The incorporation of oregano essential oil and its complexes into butter resulted in better oxidative stability compared to butter without their addition.

CONCLUSIONS. The formation of inclusion complexes by kneading and co-precipitation methodologies was confirmed by physicochemical methods and the complexation process showed positive results for antimicrobial and antioxidant activities. The incorporation of oregano essential oil and its complexes into butter was promising, ensured antimicrobial protection and oxidative stability to the product.

Keywords: *Coriandrum sativum*, *Origanum vulgare*, cyclodextrins, inclusion complex, oxidative protection.

ARTIGO I**HIDRÓLISE ENZIMÁTICA DE AROMAS CÁRNEOS PARA
EXTRAÇÃO DE COLÁGENO E OBTENÇÃO PEPTÍDEOS
BIOATIVOS**

Juliana Harumi Miyoshi^a, Thamara Thaiane da Silva Crozatti^a, Laira Machado Brandão Toller^a, Marco Aurélio Schuler Oliveira^a, Jose Uebi Maluf^b, Tieles Carina Oliveira Delani^a, Giovanni Cesar Teles^a, Eduardo Cesar Meurer^c e Graciette Matioli^{a*}

^a*State University of Maringá (UEM), Av. Colombo, 5790 - 87020-900, Maringá, PR, Brazil*

^b*BRFoods, Av. Senador Atílio Fontana, 4040, 85902-160, Toledo-PR, Brazil*

^c*Federal University of Paraná (UFPR), Advanced Campus Jandaia do Sul, 86900-000, Jandaia do Sul-PR, Brazil*

* Corresponding author: Graciette Matioli

E-mail address: gmatioli@uem.br

Orcid: <https://orcid.org/0000-0002-2531-2567>

Tel.: +55 44 3011-3868;

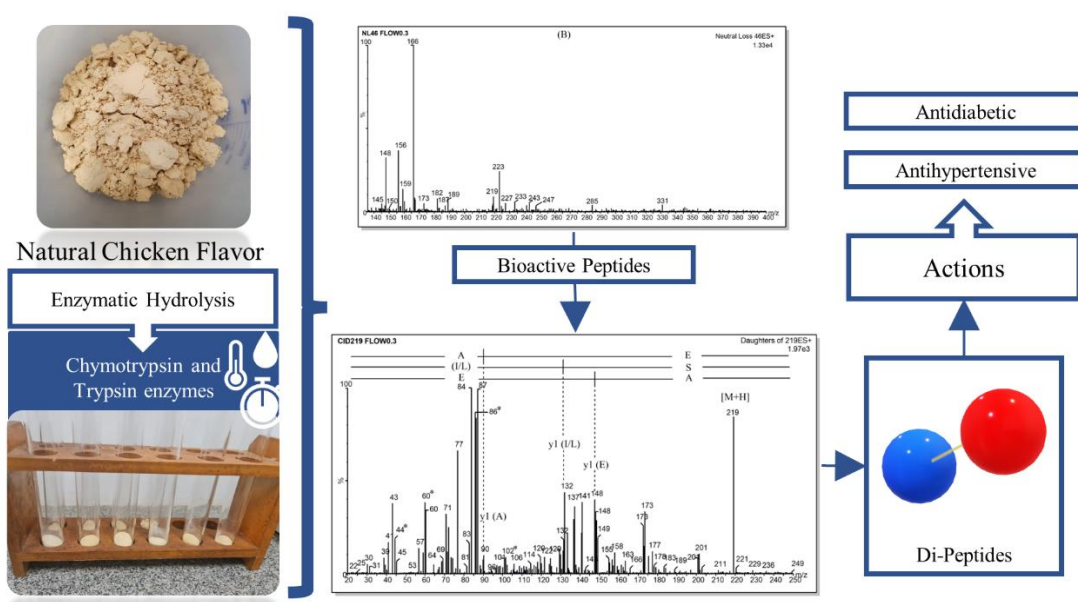
Fax: +55 44 3011-4119

RESUMO

O reaproveitamento dos subprodutos provenientes do abate de animais, como aromas cárneos, pode gerar produtos de alto valor agregado e menor impacto sobre o meio ambiente. Desses subprodutos é possível obter o colágeno, que representa 30% das proteínas de origem animal, e quando hidrolisado pode produzir peptídeos bioativos. Considerando a importância da gestão de subprodutos, a necessidade de melhorar as características funcionais de produtos industrializados e aumentar o seu valor, a presente pesquisa teve como objetivo a obtenção do colágeno de aromas cárneos com a utilização de enzimas e a avaliação dos peptídeos bioativos resultantes do processo de hidrólise. Os produtos obtidos pela ação das enzimas quimotripsina e tripsina foram secos por liofilização e determinados a proteína bruta, o grau de hidrólise e o teor de colágeno pela determinação da hidroxiprolina. Foi realizada a eletroforese em gel dos aromas e seu respectivos hidrolisados e os peptídeos bioativos obtidos foram identificados por LC-MS/MS. A quantidade de proteína bruta foi acima de 69% para o aroma de frango e seus respectivos hidrolisados, porém, para o aroma de carne, esse valor foi inferior a 20%. Na eletroforese foi observado o padrão de hidrólise das proteínas e confirmado o alto grau de hidrólise do aroma de carne. Na temperatura de 30 °C, 25% de enzima e 6 h de ensaio, o aroma de frango forneceu maior quantidade de peptídeos bioativos, na qual a prevalência de atividade foi o inibidor da dipeptidil peptidase IV, utilizado em medicamentos anti-hiperglicêmicos. Os resultados demonstraram que com o processo de hidrólise é possível obter quantidades maiores de proteína e colágeno, além da obtenção de di peptídeos com atividade biológica. Os hidrolisados bioativos dos aromas cárneos, especialmente de frango, podem ser utilizados nas indústrias farmacêutica e alimentícia, aumentando a funcionalidade do produto, bem como agregando valor aos mesmos.

Palavras-chave: biotecnologia enzimática, quimotripsina, tripsina, subprodutos cárneos, peptídeos bioativos.

Graphical Abstract



1 INTRODUÇÃO

A indústria alimentícia de carnes gera grande quantidade de subprodutos, e quando não descartados corretamente são considerados uma fonte importante de contaminação ambiental. Subprodutos de origem animal são normalmente constituídos de restos de carnes, aparas e tecido, cartilagens, sebo e ossos, os quais, podem ser submetidos à gestão, como a incineração e a reciclagem^{1,2}.

A incineração, embora possa proporcionar uma recuperação de energia pela queima dos subprodutos, apresenta elevados custos de operação e de controle de poluentes, além de recuperar baixa quantidade de energia. A reciclagem apresenta-se como melhor via de destinação, tanto por questões ambientais, quanto por questões de saúde pública e financeiras, uma vez que os subprodutos podem transformar-se em produtos comerciais com maior valor agregado, incluindo os comestíveis, semiprocessados ou destinados a outras aplicações, tais como farinhas para ração animal, produtos farmacêuticos, cosméticos, entre outros^{2,3}.

Tendo em vista que os subprodutos alimentares podem conter substâncias benéficas, como proteínas e aminoácidos, e importantes para a saúde humana, de alto valor agregado, é importante que estes sejam reaproveitados e transformados em produtos comercializáveis, os quais podem ser, por exemplo, destinados às indústrias farmacêutica e alimentícia. A utilização dos subprodutos ajudará em um menor impacto sobre o meio ambiente^{1,4,5}.

Dentre os subprodutos que tem potencial de aproveitamentos, estão os aromas de frango e carne que são geralmente obtidos por processos de cozimento, extrusão, hidrólise enzimática, entre outros. São produtos ricos em proteínas, carboidratos e lipídeos, que agregam sabor e odor natural ao alimento, que são atributos importantes para a aceitação do consumidor⁶⁻⁸. Ainda, podem ser utilizados na obtenção de produtos, como o colágeno.

O colágeno é uma proteína primária do tecido conjuntivo constituído de três cadeias polipeptídicas na forma de tríplice hélice, representando cerca de 30% das proteínas de origem animal. É considerada uma proteína chave do organismo, que assegura a coesão, elasticidade e regeneração da pele, cartilagens e ossos. Sua principal função é contribuir para a integridade estrutural da matriz extracelular, além de auxiliar na fixação celular na matriz. Ainda, apresenta propriedades mecânicas singulares, e é quimicamente inerte⁹.

A hidrólise enzimática pode ser uma possibilidade para solucionar a grande procura por processos sustentáveis para gestão dos subprodutos provenientes das indústrias de alimentos, pois gera pouco desperdício, tem-se um bom controle de processos e um maior rendimento, justificando o seu uso apesar dos altos custos¹⁰.

1 Considerando a importância da gestão dos subprodutos provenientes das indústrias de
2 alimentos para resolução de problema ambiental, a necessidade de melhorar as características
3 funcionais de produtos industrializados e desenvolvimento de produtos de alto valor agregado
4 obtidos pela química verde, a presente pesquisa teve como objetivo a utilização de enzimas para
5 obtenção do colágeno e a avaliação dos peptídeos bioativos resultantes do processo de hidrólise.

6

7 **2 MATERIAIS E MÉTODOS**

8 **2.1 Materiais**

9 **2.1.1 Reagentes e equipamentos**

10 Os principais materiais e reagentes utilizados foram: enzimas tripsina e quimotripsina
11 (Novozymes Latin America Ltda), cloreto de sódio, etanol, hidróxido de sódio, ácido clorídrico,
12 peróxido de hidrogênio, albumina bovina (padrão Sigma-Aldrich), reagente de Bradford,
13 Marcador PierceTM Unstained Protein MW (ThermoFisher Scientific), reagente de Erlich,
14 metanol, clorammina T, hidroxiprolina (padrão Sigma-Aldrich), serina (padrão Sigma-Aldrich),
15 acetonitrina (grau HPLC), água deionizada obtida pelo sistema Milli-Q (Millipore, Billerica,
16 MA). Todos os reagentes foram de grau analítico.

17 Os principais equipamentos e dispositivos utilizados foram: pipetadores, agitadores,
18 reatores de vidro encamisados, centrífuga, estufa, banho termostático, liofilizador (LIOTOP –
19 L101).

20

21 **2.1.2 Matérias primas**

22 As matérias primas Aroma Natural de Frango em pó (REF549335) e Aroma Natural de
23 Carne (REF200610 HIDRO2SP15.0) utilizadas neste projeto foram fornecidas pela empresa
24 BRFoods S/A (Brasil). As amostras foram armazenadas a 25 °C ao abrigo de luz. As análises
25 foram realizadas no Laboratório de Biotecnologia Enzimática (LaBE) da Universidade Estadual
26 de Maringá (UEM).

27

28 **2.2 Métodos**

29 **2.2.1 Hidrólise enzimática dos aromas de frango e carne para obtenção do colágeno
30 e dos peptídeos bioativos**

31 Para a extração do colágeno e peptídeos bioativos foram utilizadas as metodologias de
32 Guo *et al.*¹¹, Tang *et al.*¹², Li *et al.*¹³ e Sun *et al.*¹⁴, com modificações. Foram pesadas 20 g de
33 aroma e adicionadas 400 mL de água destilada e o pH foi ajustado e mantido em 7,5 ± 0,5
34 durante todo o processo, valor de pH de acordo com a literatura para as enzimas utilizadas.

A reação de hidrólise ocorreu em duas etapas, na qual a primeira foi realizada utilizando a enzima quimotripsina e, após, foi adicionado a enzima tripsina para iniciar a segunda etapa. Na primeira etapa foram utilizadas as temperaturas de 20, 30 e 40 °C, as concentrações de enzima variaram de 0,25, 0,50 e 0,75% com relação à massa do substrato e as reações foram realizadas nos tempos de 2, 4 e 6 h (Tabela 1).

Tabela 1: Condições estabelecidas para a primeira etapa da hidrólise enzimática.

Ensaio	Temperatura (°C)	[Enzima]/Substrato (%)	Tempo (h)
1	20	0,25	2
2	20	0,50	6
3	20	0,75	4
4	30	0,25	6
5	30	0,50	4
6	30	0,75	2
7	40	0,25	4
8	40	0,50	2
9	40	0,75	6

Após o término das reações da primeira etapa, foi adicionado ao meio reacional 0,25% da enzima tripsina, a temperatura foi ajustada para 40 °C e a reação mantida por 2 h. A reação foi interrompida colocando o meio reacional em um banho fervente por 15 min. Após esse tempo, foi utilizado banho de gelo para resfriamento do material hidrolisado e posterior centrifugação a 8000 rpm, por 30 min, a 4 °C. O sobrenadante de interesse foi liofilizado e armazenado em freezer para futura avaliação.

2.2.2 Determinação de proteína bruta pela metodologia de Micro-Kjeldahl

A determinação de proteína total foi realizada pelo método Micro-Kjeldahl^{15,16}. A proteína bruta foi dosada no material antes e depois da hidrólise nos diferentes ensaios. As amostras foram digeridas em ácido sulfúrico até 450 °C, resfriadas, adicionadas água destilada para hidratação e, posteriormente, destiladas. Após a destilação, as amostras foram tituladas com uma solução padrão de ácido clorídrico (0,5 M, fator de correção (fc)=0,972; 0,05 M, fc=1,053) para a determinação quantitativa de amônia. A % de nitrogênio determinada na amostra foi multiplicada pelo fator de conversão de nitrogênio, ou seja, para a carne é considerado o valor de 6,25.

1 **2.2.3 Eletroforese em gel SDS-PAGE**

2 Para avaliar o padrão de hidrólise de proteínas, todas as extrações foram submetidas à
3 análise por SDS-PAGE, que foi realizada de acordo com o método descrito por Laemmli¹⁷.

4 Para determinar a quantidade de amostra a ser utilizada na eletroforese em gel, foi
5 realizada a determinação de proteínas pela metodologia de Bradford (1976) utilizando albumina
6 bovina como padrão. Foi empregado 800 µL de amostra previamente diluída e 200 µL do
7 reagente de Bradford. Para o branco, foi utilizado 800 µL de água destilada. As amostras foram
8 agitadas e incubadas a temperatura ambiente por 5 min e medidas na absorbância de 595 nm.

9 As amostras foram misturadas com tampão redutor contendo 14,4 mmol/L de
10 β-mercaptoetanol, sendo que a concentração de proteína por amostra foi de 2 mg/mL. As
11 misturas com β-mercaptoetanol foram fervidas por 5 min e centrifugadas a 10.000 × g por
12 10 min. Em seguida, 10 µL da amostra foram carregados no gel de poliacrilamida. As
13 porcentagens de poliacrilamida no gel de corrida foram de 12% e de 17%. A concentração do
14 gel de empilhamento foi de 5%. Os géis foram submetidos à eletroforese a uma corrente
15 constante.

16

17 **2.2.4 Grau de hidrólise (GH) dos aromas de frango e carne**

18 O cálculo da % do grau de hidrólise (GH) dos aromas de frango e carne foi baseado na
19 metodologia de Nielsen, Petersen e Dambmann¹⁸. Para as análises, foram utilizados 400 µL do
20 padrão de serina, 400 µL de água destilada (branco) e 400 µL de cada amostra. Foram
21 adicionadas 3,0 mL da solução de o-ftaldialdeído (OPA) em cada uma das amostras e, após
22 2 min de reação, foram realizadas as leituras em espectrofotômetro na absorbância de 340 nm,
23 em triplicata. A %GH foi calculada de acordo com as equações de Adler-Nissen¹⁹.

24

25 **2.2.5 Determinação do colágeno**

26 A metodologia para quantificar o teor de colágeno foi baseada em Bergman e Loxley²⁰
27 com modificações. A proteína de colágeno possui entre seus aminoácidos a hidroxiprolina, na
28 qual atua como um marcador ideal e, desta forma, a determinação de colágeno foi realizada
29 com base na medição desse aminoácido. Foi pesado 1 g de cada amostra, adicionada de 30 mL
30 de ácido sulfúrico 3,5 mol/L por amostra e submetida a hidrólise por 16 h. O hidrolisado foi
31 transferido para um balão volumétrico de 500 mL e o volume completado com água destilada.
32 Em seguida, a solução foi filtrada. Uma alíquota do filtrado foi transferido para um balão de
33 100 mL e completado com água destilada para a quantificação da hidroxiprolina.

1 Em tubos de vidro foram adicionados 2 mL das amostras previamente preparadas e
2 adicionados 1 mL de solução oxidante contendo cloramina T e tampão citrato. Foram incubados
3 por 20 min sob agitação a 25 °C. Em seguida, foi adicionado 1 mL do reagente de Ehrlich,
4 agitados e incubados a 60 °C ao abrigo da luz. Passado esse tempo, os tubos foram arrefecidos
5 com água para posterior leitura na absorbância de 558 nm. Foi utilizada uma curva padrão de
6 hidroxiprolina.

7

8 **2.2.6 Espectrometria de Massa Sequencial (LC-MS/MS)**

9 A cromatografia líquida (LC) acoplada à espectrometria de massas (MS/MS) é uma
10 técnica muito utilizada para determinar as proteínas e seus peptídeos^{5,11,21,27}. Com o objetivo de
11 identificar di e tri peptídeos nas amostras hidrolisadas de aroma de frango e carne, o presente
12 estudo utilizou o método rápido de LC-MS/MS com espectrômetro de massa triplo-quadrupolo
13 Quattro Premier XE (Waters Corporation, Milford, MA, EUA), equipado com uma fonte de
14 ionização por eletrospray, uma bomba Waters 515 e uma coluna XBridge (Waters) C18 3,5 µm
15 (4,6 x 50 mm). Para a varredura foi realizada a perda neutra seletiva (NL) 46 Da e, em seguida,
16 a fragmentação foi efetuada por fragmentos de dissociação colisão-induzido (CID) por
17 sequenciamento *de novo*²².

18 Os aromas de frango e carne, bem como seus respectivos hidrolisados foram preparados
19 utilizando 0,1 g de amostra, suspensas em 1 mL de solução de bicarbonato de amônio 50 mM.
20 A suspensão foi agitada em vórtex por 1 min e realizado uma diluição de 1:10 em fase móvel
21 acetonitrila:água:ácido fórmico (70:30:0,1) (v/v/v). Todas as amostras foram agitadas por 1 min
22 e centrifugadas por 10 min numa rotação de aproximadamente 3000 rpm. Em seguida, as
23 amostras foram mantidas a 4 °C por 1 h. Após esse período foi realizada nova diluição de 1:10
24 utilizando a fase móvel anterior e agitadas em vórtex por 1 min.

25 A varredura e fragmentação das amostras foram conduzidas utilizando uma fonte de
26 ionização convencional por eletrospray (ESI), na qual foi operada em modo de ionização
27 positiva (ESI+) a 4,0 kV. A temperatura de dessolvatação foi de 350 °C e do gás fonte foi de
28 110 °C. A tensão do cone foi de 20 V e a energia de colisão utilizada foi de 15 V. O gás de
29 colisão utilizado na presente pesquisa foi o gás argônio numa pressão de $3,0 \times 10^{-3}$ Torr. As
30 amostras preparadas anteriormente foram injetadas no sistema LC-MS/MS em triplicata, com
31 volume de injeção de 5 µL e o tempo de execução da análise foi de 1 min para cada injeção.

32 Os resultados dos espectros foram analisados de acordo com o material descrito por
33 Cantú *et al.*²³. Após a identificação dos íons *m/z* foi realizado em triplicata o método de
34 fragmentação por dissociação induzida por colisão (CID) por sequenciamento *de novo* para

1 cada íon selecionado e, os espectros de massas foram interpretados identificando o íon imônio,
 2 os íons y1, os íons y2, os resíduos de aminoácidos confirmatórios e os íons b2. Sua
 3 funcionalidade foi aferida utilizando o banco de dados BIOPEP-UWM²⁴.

4

5 **2.2.7 Análise estatística**

6 Os resultados foram avaliados por meio de análise de variância (ANOVA) e as médias
 7 comparadas por meio do teste de Tukey, ao nível de 5% de significância.

8

9 **3 RESULTADOS E DISCUSSÃO**

10

11 **3.2 Determinação da proteína bruta dos aromas de carne e frango e seus 12 respectivos hidrolisados**

13 A proteína bruta presente no aroma de frango e carne antes do processo de hidrólise e
 14 após a ação das enzimas está apresentada na Tabela 2.

15

16 Tabela 2: Teor de proteína bruta e grau de hidrólise (%) dos aromas de frango e carne e seus
 17 respectivos hidrolisados.

Amostras	Aroma de frango		Aroma da carne	
	Proteína bruta (%)	GH (%)	Proteína bruta (%)	GH (%)
Aroma	75.3 ± 0.7 ^a	10.3 ± 0.1 ^a	19.1 ± 0.2 ^a	42.0 ± 0.7 ^a
Ensaio 1	86.7 ± 1.7 ^c	13.0 ± 0.2 ^{cef}	17.8 ± 1.0 ^a	46.1 ± 0.3 ^b
Ensaio 2	87.8 ± 0.7 ^c	13.6 ± 0.4 ^{dg}	18.4 ± 0.3 ^a	44.6 ± 0.4 ^{cb}
Ensaio 3	85.1 ± 1.4 ^c	14.1 ± 0.2 ^d	17.8 ± 0.4 ^a	44.8 ± 0.3 ^{dbc}
Ensaio 4	86.9 ± 0.2 ^c	12.7 ± 0.0 ^{cefg}	18.6 ± 0.1 ^a	44.1 ± 0.6 ^{ec}
Ensaio 5	94.0 ± 0.3 ^b	12.6 ± 0.1 ^{ef}	18.4 ± 0.4 ^a	43.6 ± 0.2 ^{fce}
Ensaio 6	88.4 ± 1.3 ^c	13.6 ± 0.1 ^{de}	17.7 ± 0.4 ^a	44.8 ± 0.1 ^{gbc}
Ensaio 7	87.2 ± 0.6 ^c	13.5 ± 0.1 ^{de}	18.7 ± 0.5 ^a	45.9 ± 0.1 ^{hb}
Ensaio 8	87.2 ± 2.9 ^c	14.9 ± 0.2 ^d	19.3 ± 0.2 ^a	42.5 ± 0.6 ^{ae}
Ensaio 9	88.5 ± 0.7 ^c	15.3 ± 0.5 ^b	19.1 ± 0.6 ^a	42.8 ± 0.6 ^{ae}

18 a, b, c, d, e, f, g, h: Médias com letras iguais na mesma coluna não diferem significativamente entre si pelo teste de Tukey
 19 ($p \leq 0,05$).

20

21 Para o aroma de frango, o teor de proteína bruta foi significativamente maior em todos
 22 os ensaios do processo de hidrólise, na qual, na temperatura de 30 °C, utilizando 0,25% da
 23 enzima quimotripsina, durante 6 h foi o ensaio que obteve melhores resultados.

24 O teor de proteína bruta do aroma de carne quando comparado com o aroma de frango
 25 foi inferior e não apresentou diferença significativa em nenhum ensaio quando comparado com
 26 seus respectivos hidrolisados (Tabela 2).

27

1 **3.3 Grau de hidrólise (GH)**

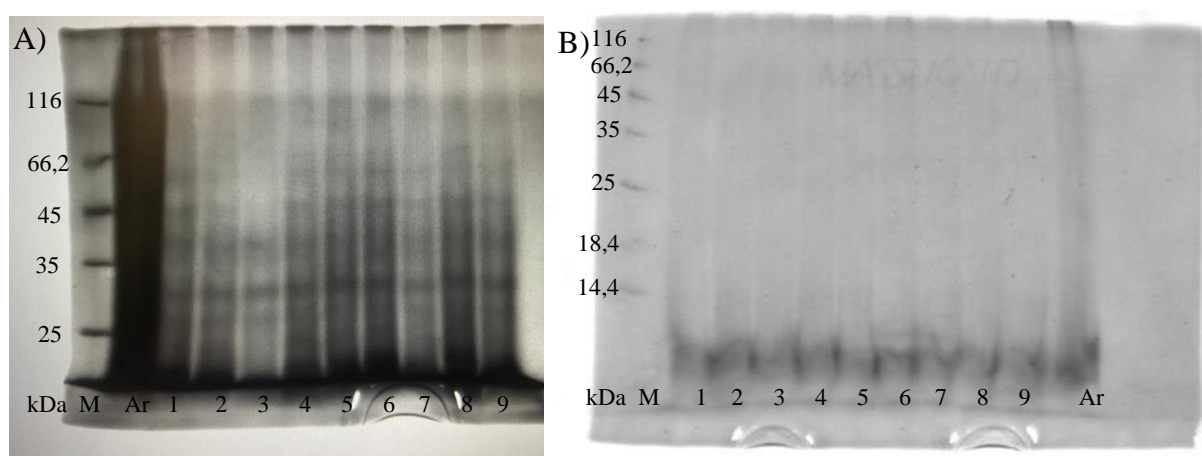
2 As propriedades bioativas dos aromas e seus hidrolisados dependem de vários fatores e
3 o GH é um dessas condições⁵. Os aromas de frango e carne fornecidos pela apresentaram um
4 %GH, na qual foi intensificado com o processo de hidrólise enzimático estudado (Tabela 2).

5 Para o aroma de frango foi observado que o processo de hidrólise enzimática aumentou
6 significativamente a em todos os ensaios, sendo que o ensaio 9, utilizando a temperatura de 40
7 °C, 0,75% da enzima quimotripsina, com tempo de reação de 6 h, apresentou maior %GH grau
8 de hidrólise. Para o aroma de carne, os resultados também indicam uma diferença significativa
9 para os hidrolisados, exceto nos ensaios 8 e 9, nos quais foram utilizadas as maiores
10 temperaturas e maiores concentrações de enzima. Zhang, Li e Shi²⁵ relataram que produtos já
11 hidrolisados sofrem uma menor influência de enzimas, o que pode ser observado no presente
12 estudo, na qual o %GH dos hidrolisados aumentou no máximo 5% para o aroma de frango e
13 4% para o aroma de carne.

14

15 **3.4 Eletroforese em gel (SDS-PAGE)**

16 Os resultados da eletroforese em gel são apresentados na Figura 2. Para o aroma de
17 frango e seus respectivos hidrolisados foram utilizados o gel de empilhamento de 12%. Para o
18 aroma de carne, o mesmo gel não apresentou banda e foi utilizado um gel de empilhamento de
19 maior concentração, ou seja, 17%. Para os aromas de frango e carne são observados no gel uma
20 banda arrastada (Ar), na qual pode sugerir que as amostras já possuíam certo grau de hidrólise.



22

23 Figura 1: Gel de poliacrilamida (SDS-PAGE) obtido de amostras hidrolisadas e não
24 hidrolisadas de (A) frango e (B) carne utilizando diferentes parâmetros de temperatura,
25 concentração da enzima quimotripsina e tempo de reação (Tabela 1: ensaios 1-9). M: Marcador
26 Pierce™ Unstained Protein MW (ThermoFisher Scientific). Ar: Aroma.

1 Para os produtos das hidrolises dos aromas foi observado bandas mais intensas na região
 2 final do gel, indicando a existência de fragmentos menores que 25 e 10 kDa para o aroma de
 3 frango e carne, respectivamente. Sendo assim, após a utilização das enzimas quimotripsina e
 4 tripsina neste estudo, os produtos obtidos sofreram uma maior fragmentação.

5 É possível sugerir que os resultados apresentados no SDS-PAGE se relacionam com os
 6 observados no GH. Ou seja, para o aroma de carne não foi observado bandas de proteínas
 7 mesmo em géis mais concentrados, sugerindo, novamente, que os mesmos já se apresentavam
 8 hidrolisados e que seus produtos obtidos nos ensaios de 1 a 9 tiveram sua hidrólise intensificada.
 9

10 **3.5 Dosagem do colágeno pela determinação do teor de hidroxiprolina**

11 O teor de colágeno (%) nos aromas de frango e de carne, bem como o dos seus
 12 respectivos hidrolisados, está apresentado na Tabela 3.

14 Tabela 3: Teor de colágeno (%) determinado pela quantificação de hidroxiprolina.

Amostra	Aroma de frango	Aroma de carne
	Colágeno (%)	Colágeno (%)
Aroma	23.3 ± 0.3 ^a	4.0 ± 0.5 ^{abc}
Ensaio 1	28.9 ± 0.3 ^b	2.9 ± 0.1 ^{bc}
Ensaio 2	29.0 ± 0.9 ^b	2.9 ± 0.1 ^{cb}
Ensaio 3	27.9 ± 0.5 ^b	3.1 ± 0.1 ^{abc}
Ensaio 4	28.4 ± 0.5 ^b	3.3 ± 0.1 ^{abc}
Ensaio 5	28.7 ± 0.3 ^b	3.3 ± 0.1 ^{abc}
Ensaio 6	27.5 ± 2.4 ^b	3.2 ± 0.2 ^{abc}
Ensaio 7	27.7 ± 0.5 ^b	3.5 ± 0.1 ^{abc}
Ensaio 8	27.3 ± 0.8 ^b	4.3 ± 0.9 ^a
Ensaio 9	27.8 ± 0.6 ^b	3.7 ± 0.1 ^{abc}

15 ^{a, b, c:} Médias com letras iguais na mesma coluna não diferem significativamente entre si pelo teste de Tukey
 16 ($p \leq 0,05$).
 17

18 O aroma de frango apresentou um teor de colágeno significativamente menor que
 19 aqueles obtidos por seus hidrolisados. Porém, as amostras dos hidrolisados não apresentaram
 20 diferenças significativas entre elas, ou seja, as variações dos parâmetros de temperatura,
 21 concentração de enzima e tempo de reação estudados nesta pesquisa não alteraram o processo
 22 de hidrólise (Tabela 3).

23 O aroma de carne e seus respectivos hidrolisados não apresentaram diferenças
 24 significativas entre eles, sendo assim, o processo de hidrólise não foi favorável para obtenção
 25 de colágeno nesta amostra (Tabela 3).
 26

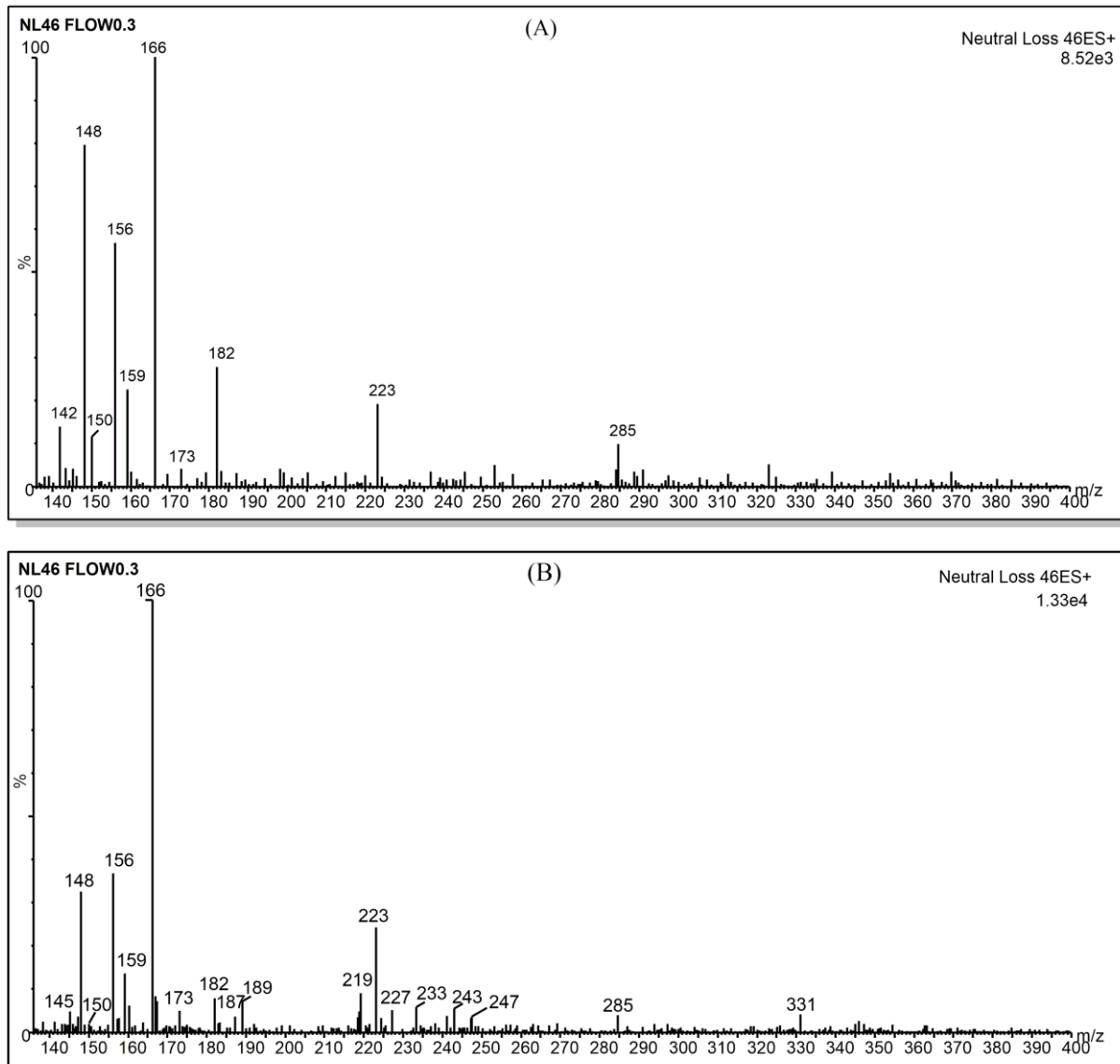
27 **3.6 Identificação dos peptídeos bioativos por LC-MS/MS**

1 As análises de varredura foram realizadas nas amostras de aroma de frango e de carne
2 para avaliar se os mesmos apresentavam peptídeos bioativos e identificar as possíveis alterações
3 desses peptídeos após a hidrólise enzimática. Em todas as amostras foram observados picos
4 bem formados.

5 Na varredura completa, para os aromas de frango e carne, os íons identificados
6 utilizando as razões m/z com intensidade suficiente para fragmentar (intensidade absoluta
7 próxima de 1000) estão na Figura 3 e Tabela 4. Os íons escolhidos para a fragmentação foram
8 os de massas acima de m/z 200, sendo assim, foram fragmentados os íons de m/z 223 e m/z 285
9 do aroma de frango e os íons de m/z 219, m/z 223, m/z 227, m/z 233, m/z 243, m/z 247, m/z 285
10 e m/z 331 do aroma de carne. Também foi possível observar que o aroma de carne apresentou
11 uma maior quantidade de íons na varredura completa indicando mais uma vez a alta %GH da
12 amostra.

13

14



2
3 Figura 2: Espectro de massa por cromatografia líquida (LC-MS/MS) perda de massa neutra de
4 46 Da de (A) Aroma de frango e (B) Aroma de carne.
5
6

1 Tabela 4: Íons identificados na varredura completa, para os hidrolisados de aroma de frango e
 2 carne utilizando os íons m/z .

Amostras	Aroma de frango	Aroma de carne
Ensaio 1	148, 150, 156, 166, 167, 176, 182, 189, 223 e 227.	148, 150, 156, 159, 166, 173, 182, 187, 189, 219, 223, 227 e 243.
Ensaio 2	142, 148, 150, 156, 166, 167, 182, 189, 221, 223, 227 e 285.	145, 148, 150, 156, 159, 166, 173, 182, 187, 189, 219, 223, 227 e 243.
Ensaio 3	142, 146, 148, 150, 156, 166, 182, 189, 219, 221, 223, 227 e 285.	148, 150, 156, 159, 166, 173, 182, 189, 219, 223, 227, 243, 247 e 347.
Ensaio 4	142, 146, 148, 150, 156, 166, 182, 189, 219, 221, 223, 227 e 285.	148, 150, 156, 159, 166, 173, 182, 187, 189, 215, 219, 223, 227, 233, 243 e 247.
Ensaio 5	142, 148, 150, 156, 166, 175, 182, 189, 206, 219, 221, 223, 227, 233 e 285.	148, 150, 156, 159, 166, 182, 189, 219, 223, 227, 243, 247 e 347.
Ensaio 6	148, 150, 156, 166, 182, 189, 206, 219, 223, 227, 234 e 285.	148, 150, 156, 159, 166, 173, 182, 187, 189, 219, 223 e 243.
Ensaio 7	142, 148, 150, 156, 166, 167, 182, 189, 206, 221, 223 e 227.	148, 150, 156, 159, 166, 182, 189, 219, 223, 227, 233, 243, 245 e 247.
Ensaio 8	142, 146, 148, 150, 156, 166, 167, 182, 189, 206, 223, 227 e 272.	148, 150, 156, 159, 166, 171, 182, 189, 219, 223, 227, 243, 247, 269 e 285.
Ensaio 9	148, 150, 156, 166, 167, 182, 189, 206 e 223.	148, 150, 156, 159, 166, 182, 187, 189, 215, 219, 223, 227, 243, 247, 289 e 294.

3
 4 Para o aroma de frango não foram observados íons nos espectros de fragmentação dos
 5 íons m/z de 223 e 285. Com relação ao aroma de carne, o espectro de fragmentação do íon de
 6 m/z 219 apresentou três valores diferentes de y_1 (Figura 4). O primeiro valor encontrado de y_1
 7 foi 90, correspondente ao aminoácido alanina (A), o resíduo calculado foi de 129 equivalente
 8 ao ácido glutâmico (E), sendo assim, a sequência peptídica formada foi EA confirmado pelos
 9 íons imônios 102 e 44 presentes no espectro de fragmentação. A atividade biológica do
 10 dipeptídeo EA são duas, sendo elas a inibição da enzima conversora de angiotensina (ECA) e
 11 inibidor da alfa-glicosidase²⁴. Os demais resultados obtidos a partir da fragmentação dos íons
 12 m/z do hidrolisado de frango, do aroma de carne e seus respectivos hidrolisados foram
 13 interpretados conforme análise acima e estão apresentados na Tabela 5, bem como suas
 14 atividades biológicas baseadas no banco de dados BIOPEP-UWM²⁴. É válido salientar que no
 15 processo de hidrólise não foi obtido tri peptídeos para nenhuma das amostras.

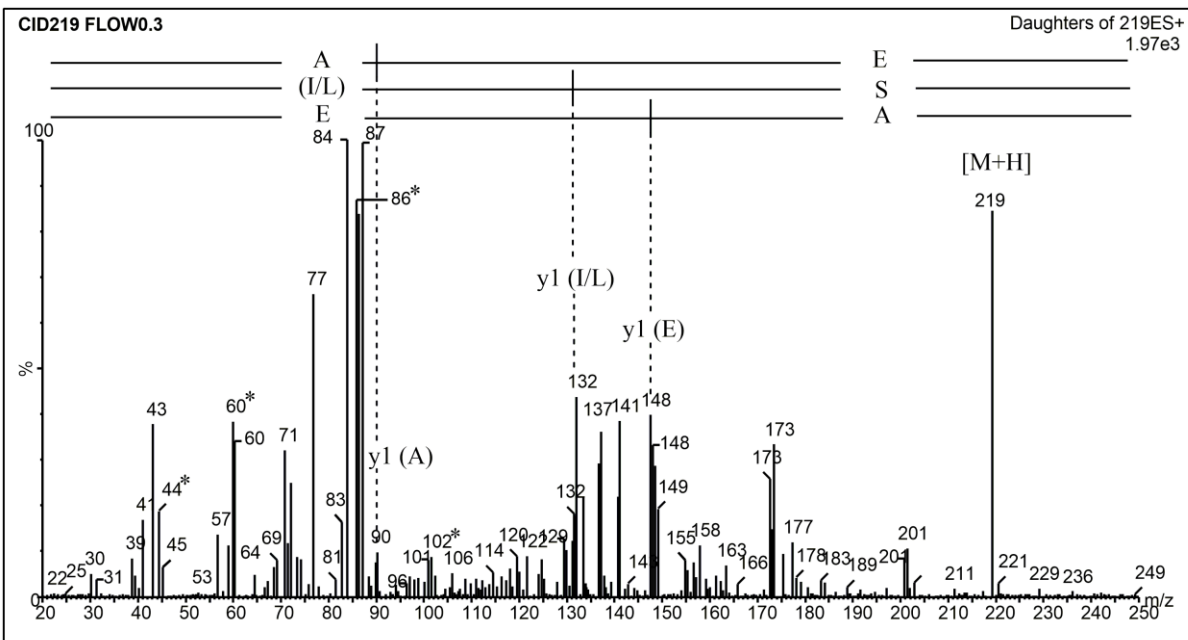


Figura 3: Espectro de massa da etapa de fragmentação para sequenciamento *de novo* para o íon m/z 219 do aroma de carne. (*) representa os íons de amônio do aminoácido confirmados.

4

1 Quadro 1: Peptídeos identificados por LC-MS/MS no aroma de frango e de carne e seus respectivos hidrolisados.*

Amostra	(M+H)	y1	Resíduo	Íon Imônio	Sequência	Atividade biológica**
Aroma (Frango)	-	-	-	-	-	-
Ensaio 1 (Frango)	223	166 (F)	57 (G)	30 (G); 120 (F)	GF	Inibidor da ECA; Inibidor da dipeptidil peptidase IV (DPP IV); Inibidor da DPP III
	223	120 (T)	103 (C)	74 (T); 76 (C)	CT	-
	227	90 (A)	137 (H)	110 (H)	HA	Inibidor da DPP IV
	227	156 (H)	71 (A)	110 (H)	AH	Inibidor da ECA; Inibidor da DPP IV
Ensaio 2 (Frango)	223	166 (F)	57 (G)	120 (F)	GF	Inibidor da ECA; Inibidor da DPP IV; Inibidor da DPP III
	227	156 (H)	71 (A)	110 (H)	AH	Inibidor da ECA; Inibidor da DPP IV
Ensaio 3 (Frango)	223	166 (F)	57 (G)	30 (G); 120 (F)	GF	Inibidor da ECA; Inibidor da dipeptidil peptidase IV (DPP IV); Inibidor da DPP III
	223	120 (T)	103 (C)	76 (C)	CT	-
	227	90 (A)	137 (H)	110 (H)	HA	Inibidor da DPP IV
Ensaio 4 (Frango)	223	166 (F)	57 (G)	30 (G); 120 (F)	GF	Inibidor da ECA; Inibidor da dipeptidil peptidase IV (DPP IV); Inibidor da DPP III
	223	120 (T)	703 (C)	74 (T)	CT	-
	227	90 (A)	137 (H)	44 (A); 110 (H)	HA	Inibidor da DPP IV
	227	156 (H)	71 (A)	44 (A); 110 (H)	AH	Inibidor da ECA; Inibidor da DPP IV
	219	132 (I/L)	87 (S)	60 (S); 86 (I/L)	S(I/L)	Inibidor da DPP IV; Regulador da atividade da fosfoglicerato quinase
	219	148 (E)	71 (A)	44 (A); 102 (E)	AE	Inibidor da DPP IV
	221	90 (A)	131 (M)	44 (A); 104 (M)	MA	Inibidor da DPP IV
	221	120 (T)	101 (T)	74 (T)	TT	Inibidor da DPP IV
	221	150 (M)	71 (A)	44 (A); 104 (M)	AM	-
	219	90 (A)	129 (E)	44 (A); 102 (E)	EA	Inibidor da ECA; Inibidor da alfa-glicosidase
	219	106 (S)	113 (I)	60 (S); 86 (I)	IS	-
	219	118 (V)	101 (T)	72 (V); 74 (T)	TV	Inibidor da DPP IV
	219	120 (T)	99 (V)	72 (V); 74 (T)	VT	Inibidor da DPP IV

*Continua. **Atividade biológica identificada pela base de dados BIOPEP-UWM²⁴.

1 Quadro 1: Peptídeos identificados por LC-MS/MS no aroma de frango e de carne e seus respectivos hidrolisados.*

Amostra	(M+H)	y1	Resíduo	Íon Imônio	Sequência	Atividade biológica**
Ensaio 5 (Frango)	223	166 (F)	57 (G)	30 (G); 120 (F)	GF	Inibidor da ECA; Inibidor da DPP IV; Inibidor da DPP III
	233	132 (I/L)	101 (T)	74 (T); 86 (I/L)	T(I/L)	Inibidor da DPP IV
Ensaio 6 (Frango)	223	166 (F)	57 (G)	120 (F)	GF	Inibidor da ECA; Inibidor da DPP IV; Inibidor da DPP III
	227	90 (A)	137 (H)	44 (A); 110 (H)	HA	Inibidor da DPP IV
	227	156 (H)	71 (A)	44 (A); 110 (H)	AH	Inibidor da ECA; Inibidor da DPP IV
Ensaio 7 (Frango)	223	166 (F)	57 (G)	30 (G); 120 (F)	GF	Inibidor da ECA; Inibidor da DPP IV; Inibidor da DPP III
Ensaio 8 (Frango)	223	166 (F)	57 (G)	30 (G); 120 (F)	GF	Inibidor da ECA; Inibidor da DPP IV; Inibidor da DPP III
	272	175 (R)	97 (P)	70 (P); 129 (R)	PR	Inibidor da ECA; Inibidor da DPP III
Ensaio 9 (Frango)	223	166 (F)	57 (G)	30 (G); 120 (F)	GF	Inibidor da ECA; Inibidor da DPP IV; Inibidor da DPP III
Aroma (Carne)	223	166 (F)	57 (G)	120 (F)	GF	Inibidor da ECA; Inibidor da dipeptidil peptidase IV (DPP IV); Inibidor da DPP III
	219	132 (I/L)	87 (S)	60 (S); 86 (I/L)	S(I/L)	Inibidor da DPP IV; Regulador da atividade da fosfoglicerato quinase
	219	148 (E)	71 (A)	44 (A); 102 (E)	AE	Inibidor da DPP IV
	219	90 (A)	129 (E)	44 (A); 102 (E)	EA	Inibidor da ECA; Inibidor da alfa-glicosidase
	233	132 (I/L)	101 (T)	74 (T); 86 (I/L)	T(I/L)	Inibidor da DPP IV
	247	148 (E)	99 (V)	72 (V); 102 (E)	VE	Inibidor da ECA; Inibidor da DPP IV; Inibidor da alfa-glicosidase
Ensaio 1 (Carne)	227	90 (A)	137 (H)	44 (A); 110 (H)	HA	Inibidor da DPP IV
	227	156 (H)	71 (A)	44 (A); 110 (H)	AH	Inibidor da ECA; Inibidor da DPP IV
Ensaio 2 (Carne)	227	156 (H)	71 (A)	44 (A); 110 (H)	AH	Inibidor da ECA; Inibidor da DPP IV

2 *Continua. **Atividade biológica identificada pela base de dados BIOPEP-UWM²⁴.

1 Quadro 1: Peptídeos identificados por LC-MS/MS no aroma de frango e de carne e seus respectivos hidrolisados.

Amostra	(M+H)	y1	Resíduo	Íon Imônio	Sequência	Atividade biológica**
Ensaio 3 (Carne)	247	148 (E)	99 (V)	72 (V); 102 (E)	VE	Inibidor da ECA; Inibidor da DPP IV; Inibidor da alfa-glicosidase
	247	116 (P)	131 (M)	70 (P)	MP	Inibidor da DPP IV
	247	133 (N)	114 (N)	87 (N)	NN	Inibidor da DPP IV
	247	134 (D)	113 (I/L)	86 (I/L); 88 (D)	(I/L)D	-
Ensaio 4 (Carne)	215	116 (P)	99 (V)	70 (P)	VP	Inibidor da ECA; Inibidor da DPP IV
	215	118 (V)	97 (P)	70 (P)	PV	Inibidor da DPP IV
Ensaio 5 (Carne)	247	148 (E)	99 (V)	72 (V)	VE	Inibidor da ECA; Inibidor da DPP IV; Inibidor da alfa-glicosidase
Ensaio 6 (Carne)	-	-	-	-	-	-
Ensaio 7 (Carne)	245	132 (I/L)	113 (I/L)	86 (I/L)	(I/L)(I/L)	Peptídeo estimulante da captação de glicose; Inibidor da DPP IV; Inibidor da ECA; Neuropeptídeo
	247	150 (M)	97 (P)	104 (M)	PM	Inibidor da DPP IV; Inibidor da ECA
Ensaio 8 (Carne)	219	120 (T)	99 (V)	74 (T)	VT	Inibidor da DPP IV
	219	132 (I/L)	87 (S)	60 (S); 86 (I/L)	S(I/L)	Inibidor da DPP IV; Regulador da atividade da fosfoglicerato quinase
	219	148 (E)	71 (A)	102 (E)	AE	Inibidor da DPP IV
	247	148 (E)	99 (V)	72 (V)	VE	Inibidor da ECA; Inibidor da DPP IV; Inibidor da alfa-glicosidase
Ensaio 9 (Carne)	219	148 (E)	71 (A)	102 (E)	AE	Inibidor da DPP IV
	219	90 (A)	129 (E)	102 (E)	EA	Inibidor da ECA; Inibidor da alfa-glicosidase
	215	116 (P)	99 (V)	70 (P); 72 (V)	VP	Inibidor da ECA; Inibidor da DPP IV
	247	132 (I/L)	115 (D)	86 (I/L); 88 (D)	D(I/L)	Inibidor da ECA

2 **Atividade biológica identificada pela base de dados BIOPEP-UWM²⁴.

3

4 Portanto, a partir dos resultados obtidos para o aroma de frango e seus respectivos hidrolisados
5 (Tabela 5) foi possível observar que o processo de hidrólise enzimática favoreceu a quebra das
6 proteínas presente no substrato transformando-as em di peptídeos com atividade biológica. O ensaio
7 que promoveu maior variedade de peptídeos bioativos foi o ensaio 4, na qual a reação com a enzima
8 quimotripsina foi na temperatura de 30 °C, utilizando 0,25% de enzima, por 6 h, gerando 13 di
9 peptídeos identificados. Com relação à bioatividade dos peptídeos, foi observado que a atividade
10 prevalente é a inibição da ECA.

11 Para o aroma de carne foi verificado que o processo de hidrólise não favoreceu a obtenção de
12 peptídeos biologicamente ativos, uma vez que o aroma de carne sem hidrólise já havia apresentado
13 uma variedade maior desses peptídeos. Também foi observado que em alguns ensaios o processo de
14 hidrólise alterou os di peptídeos presentes no aroma de carne sem hidrólise, sugerindo que os mesmos
15 foram hidrolisados no processo e outros foram formados. As principais bioatividades dos peptídeos
16 do aroma de carne e seus respectivos hidrolisados encontrados no banco de dados BIOPEP foram a
17 inibição da ECA e inibição da DPP IV (Tabela 5).

18 Na revisão publicada por Susanto, Fadlilah e Amin²⁶, com a utilização das enzimas, como a
19 tripsina e quimotripsina, foi obtido peptídeos bioativos com atividade de inibição da ECA a partir da
20 hidrólise das proteínas da carne. Os peptídeos inibidores da ECA e da DPP IV estão diretamente
21 ligados as atividades anti-hipertensiva e antidiabética, respectivamente, e esses peptídeos ao serem
22 utilizados nas indústrias farmacêuticas e alimentícias adicionam propriedades funcionais, os quais
23 agregam valor ao produto²⁷.

24

25 **4 Conclusão**

26 O processo de hidrólise utilizando as enzimas quimotripsina e tripsina proporcionou para o
27 aroma de frango um maior teor de proteína e, consequentemente, uma maior quantidade de colágeno.
28 A eletroforese em gel (SDS-PAGE) confirmou a eficiência do processo de hidrolise, mostrando a
29 diminuição do tamanho das proteínas presentes nas amostras, bem como o alto %GH do aroma de
30 carne.

31 A metodologia inovadora utilizada por LC-MS/MS para os peptídeos hidrolisados
32 enzimaticamente resultou na identificação de di peptídeos, na qual, as propriedades bioativas
33 identificadas pelo banco de dados BIOPEP-UWM foram de inibição da ECA, inibição da DPP III e
34 IV, inibidor da alfa-glicosidase e regulador da atividade da fosfoglicerato quinase.

35 Portanto, esta pesquisa mostrou que a aplicação da biotecnologia enzimática é uma escolha
36 promissora para agregar valor a um subproduto da indústria, como os aromas, melhorando suas
37 características tecnológicas, como solubilidade e funcionais.

38

39

40 REFERÊNCIAS BIBLIOGRÁFICAS

- 41 1. Barros, f. D.; Licco, E. A. Revista Nacional da Carne **2007**, 166-171.
- 42 2. Wang, X.; Shen, Q.; Zhang, C.; Jia, W.; Han, L.; Yu, Q.; *Carbohydr Polym* **2019**, 207, 191.
43 [https://doi.org/10.1016/j.carbpol.2018.11.086]
- 44 3. Girotto, F.; Alibardi, L.; Cossu, R.; *Waste Management* **2015**, 45, 32.
45 [https://doi.org/10.1016/j.wasman.2015.06.008]
- 46 4. Hamed, I.; Özogul, F.; Regenstein, J. M.; *Trends Food Sci Technol* **2016**, 48, 40.
47 [https://doi.org/10.1016/j.tifs.2015.11.007]
- 48 5. Cao, C.; Xiao, Z.; Ge, C.; Wu, Y.; *Crit Rev Food Sci Nutr* **2022**, 62, 8703.
49 [https://doi.org/10.1080/10408398.2021.1931807]
- 50 6. Ran, X. L.; Zhang, M.; Wang, Y.; Liu, Y.; *Drying Technology* **2019**, 37, 373.
51 [https://doi.org/10.1080/07373937.2018.1458734]
- 52 7. Xu, J.; Zhang, M.; Wang, Y.; Bhandari, B.; *Food Reviews International* **2023**, 39, 802.
53 [https://doi.org/10.1080/87559129.2021.1926480]
- 54 8. Fan, H.; Zhang, M.; Mujumdar, A. S.; Liu, Y.; *Drying Technology* **2021**, 39, 1240.
55 [https://doi.org/10.1080/07373937.2021.1894440]
- 56 9. Silva TF, Penna ALB. Rev Inst Adolfo Lutz **2012**; 71 (3), 530-9.
- 57 10. Schmidt, M. M.; Dornelles, *; Mello, R. O.; Kubota; Mazutti, M. A.; Kempka; Demiate, I. M.;
58 *Int Food Res J* **2016**, 23.
- 59 11. Guo, L.; Hou, H.; Li, B.; Zhang, Z.; Wang, S.; Zhao, X.; *Process Biochemistry* **2013**, 48, 988.
60 [https://doi.org/10.1016/j.procbio.2013.04.013]
- 61 12. Tang, C. H.; Wang, X. S.; Yang, X. Q.; *Food Chem* **2009**, 114, 1484.
62 [https://doi.org/10.1016/j.foodchem.2008.11.049]
- 63 13. Li, W.; Kobayashi, T.; Meng, D. W.; Miyamoto, N.; Tsutsumi, N.; Ura, K.; Takagi, Y.; *Food
64 Biosci* **2021**, 41, [https://doi.org/10.1016/j.fbio.2021.100991]
- 65 14. Sun, B.; Li, C.; Mao, Y.; Qiao, Z.; Jia, R.; Huang, T.; Xu, D.; Yang, W.; *Int J Food Sci Technol*
66 **2021**, 56, 3443. [https://doi.org/10.1111/ijfs.14968]
- 67 15. Silva, D. Jorge.; Queiroz, A. C. de; *Análise de alimentos : métodos químicos e biológicos*; 3 ed.;
68 2002: Viçosa, **2002**
- 69 16. DETMANN, E.; COSTA E SILVA, L. F.; ROCHA, G. C.; PALMA, M. N. N.; RODRIGUES,
70 J. P. P.; *Métodos para análise de alimentos: INCT - ciência animal.*; 2 ed.; Visconde Rio Branco,
71 **2021**
- 72 17. LAEMMLI, U. K.; *Nature* **1970**, 227, 680. [https://doi.org/10.1038/227680a0]

- 73 18. Nielsen, P. M.; Petersen, D.; Dambmann, C.; *Food Chemistry and Toxicology JFS: Food*
74 *Chemistry and Toxicology* **2001**, 66.
- 75 19. Adler-Nissen, J.; *Journal of Chemical Technology and Biotechnology. Biotechnology* **1984**, 34,
76 215. [<https://doi.org/10.1002/jctb.280340311>]
- 77 20. Bergman, M.; Loxley, R.; *Anal Chem* **1963**, 35, 12, 1961–1965.
78 [<https://doi.org/10.1021/ac60205a053>]
- 79 21. Abraham, L. C.; Zuena, E.; Perez-Ramirez, B.; Kaplan, D. L.; *J Biomed Mater Res B Appl*
80 *Biomater* **2008**, 87, 264. [<https://doi.org/10.1002/jbm.b.31078>]
- 81 22. Poliseli, C. B.; Tonin, A. P. P.; Martinez, F. C.; Nascimento, N. C. do; Braz, V.; Maluf, J.;
82 Ribeiro, V. M. S.; Della Rosa, F. A.; Souza, G. H. M. F.; Meurer, E. C.; *Journal of Mass*
83 *Spectrometry* **2021**, 56, [<https://doi.org/10.1002/jms.4701>]
- 84 23. Cantú, M. D.; Carrilho, E.; *Química Nova* **2008**, 31, 669-675.
85 [<https://www.researchgate.net/publication/262545847>]
- 86 24. Minkiewicz; Iwaniak; Darewicz; *Int J Mol Sci* **2019**, 20, 5978.
87 [<https://doi.org/10.3390/ijms20235978>]
- 88 25. Zhang, Z.; Li, G.; Shi, B.; *Journal of The Society of Leather Technologists and Chemists* **2006**,
89 90, 23. <https://api.semanticscholar.org/CorpusID:41763002>
- 90 26. Susanto, E.; Fadlilah, A.; Fathul Amin, M.; *IOP Conf Ser Earth Environ Sci* **2021**, 888
91 [<https://doi.org/10.1088/1755-1315/888/1/012058>]
- 92 27. da Silva Crozatti, T. T.; Miyoshi, J. H.; Tonin, A. P. P.; Tomazini, L. F.; Oliveira, M. A. S.;
93 Maluf, J. U.; Meurer, E. C.; Matioli, G.; *Int J Food Sci Technol* **2023**, 58, 1586.
94 [<https://doi.org/10.1111/ijfs.15886>]
- 95
- 96

97

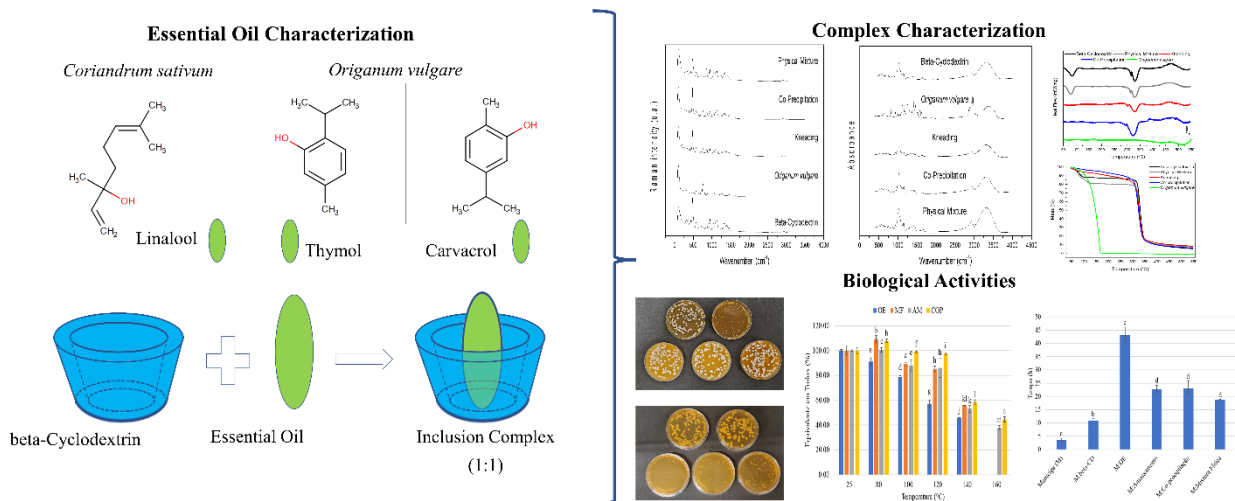
ARTIGO II

98

99

100

101

Food Hydrocolloids**Graphical Abstract (GA)**

102

103 **Complexation of essential oils with beta-cyclodextrin: characterization of complexes,**
104 **determination of antimicrobial, antioxidant activities and application**

105

106

107 *Juliana Harumi Miyoshi^a, Thamara Thaiane da Silva Crozatti^a, Júlia Rosa de Brito^a, Henrique*
108 *dos Santos^a, Juliana Cristina Castro^a, Francielle Sato^a, Leandro Herculano da Silva^b, Ana*
109 *Claudia Nogueira Mulati^c, Gislaine Franco de Moura Costa^a e Graciette Matioli^{a*}*

110

111

112 ^a*State University of Maringá (UEM), Av. Colombo, 5790 - 87020-900, Maringá, PR, Brazil*

113 ^b*Federal Technological University of Paraná (UTFPR), Campus Medianeira, 85884-000,*
114 *Medianeira-PR, Brazil*

115 ^c*Federal University of Paraná (UFPR), Advanced Campus Jandaia do Sul, 86900-000, Jandaia do*
116 *Sul-PR, Brazil*

117

118

119

120

121

122 * Corresponding author: Graciette Matioli

123 E-mail address: gmatioli@uem.br

124 Orcid: <https://orcid.org/0000-0002-2531-2567>

125 Tel.: +55 44 3011-3868;

126 Fax: +55 44 3011-4119

127

128

Abstract

129

130 Coriander and oregano essential oils (EOs) have chemical and bioactive properties, however, they
131 have limited applicability due to low solubility and instability. This research aimed to complex EOs
132 with beta-cyclodextrin, characterize the inclusion complexes (IC), evaluate antioxidant and
133 antimicrobial activities and incorporation into food product. The major compounds in coriander and
134 oregano EOs were linalool and carvacrol, respectively. Using the characterization techniques, it was
135 possible to strongly suggest the formation of OE-beta-Cyclodextrin IC. Oregano EO showed an
136 ABTS⁺ radical scavenging activity of 1836.33 µmol/mg of Trolox and in the antioxidant stability
137 assay at different temperatures, the free EO had its activity drastically reduced, while the complexes
138 remained stable. Agar diffusion methodology proved that encapsulation improved antimicrobial
139 activity. The use of oregano EO and its complexes in butter was characterized by the Rancimat
140 method and showed oxidative protection, being promising in the development of innovative products
141 with EOs. It is concluded that the methodologies used were adequate for confirming the complexes
142 of EOs with beta-CD, and that the complexation contributed to the antioxidant stability and increased
143 antimicrobial activity of the EOs evaluated, validating their use in medicines, cosmetics and foods
144 during the production, transport and marketing.

145

146 **Keywords:** *Coriandrum sativum*, *Origanum vulgare*, cyclodextrins, inclusion complex, oxidative
147 protection.

148

149 **1 Introduction**

150 Essential oils (EOs) have a complex variety in chemical composition, presenting diverse
151 properties, such as antimicrobial, antifungal, antioxidant potential, antitumor, anti-inflammatory
152 action, between others. Due to this plurality of compounds and activities, they are being widely used
153 in various products in different industrial sectors. Most EOs are regulated by the Food and Drug
154 Administration (FDA) and generally recognized as safe or “GRAS”. In the food industry, they are
155 used to provide sensory and preservative characteristics. In the pharmaceutical industry they are used
156 as phytotherapeutics and in dental products as anti-inflammatories and antiseptics. In the cosmetics
157 industry they provide benefits such as repellent, antioxidant and fragrance (Kfouri et al., 2016;
158 Răileanu et al., 2013; Vishwakarma et al., 2016).

159 Coriander (*Coriandrum sativum*) is a spice that has flavoring, medicinal and nutritional
160 properties. Several studies have identified in its EO an antibacterial, antioxidant, herbicide and
161 anticancer activity, among others. Additionally, it can be used to prevent the formation of biofilms
162 on food. It is an EO widely used in the food and cosmetics industries. Monoterpenes and hydrocarbons
163 are generally found in its chemical composition, such as linalool (Kačániová et al., 2020; Sumalan et
164 al., 2019).

165 Oregano (*Origanum vulgare*) has a high amount of bioactive compounds beneficial to health.
166 Its EO has been documented for a long time and demonstrates good results in relation of inhibitory
167 capacity against various gram-positive and gram-negative bacteria. Its extraction is made from the
168 plant's leaves and its oil is made up of a variety of chemical components, mainly carvacrol and thymol,
169 with proven antimicrobial activity and high stability (Gruľová et al., 2020; Khafaga et al., 2020;
170 Lombrea et al., 2020).

171 The application of EOs is limited due to their low solubility in aqueous media (Rodrigues et
172 al., 2017). In addition, EOs are unstable and vulnerable to degradation by light, heat, temperature,
173 among others. The microencapsulation, using complexing agents, such as cyclodextrins (CDs),
174 facilitates the solubilization of EOs in aqueous media, increasing their stability, with preservation of
175 its antioxidant activity and improved bioavailability (Kfouri et al., 2015; Răileanu et al., 2013).

176 CDs are cyclic molecules produced by the enzyme cyclomaltodextrin glucanotransferase
177 (CGtase) through the intramolecular transglycosylation reaction of starch, in which glucose
178 molecules are linked by α -1,4-glycosidic bonds. Thus, they form a truncated cone containing six,
179 seven and eight glucose molecules, called alpha-CD, beta-CD and gamma-CD, respectively. These
180 oligosaccharides have a series of applications, highlighting the ability to complex molecules within
181 their hydrophobic cavity. With a cavity that can host molecules with masses ranging from 200 to 800
182 g/mol, beta-CD is the most used, in addition to having a lower cost compared to other CDs. The
183 encapsulation directly affects the physicochemical properties of the complexed molecule, increasing

184 solubility and stability in the presence of light, heat or oxidation and decreasing the volatility of the
185 compound. Therefore, the application of cyclodextrins has increased, mainly in the areas of food,
186 medicine, perfumery and agriculture (Liu et al., 2022; Panda et al., 2022).

187 Considering the great functionality of EOs and the need to stabilize and solubilize them to
188 enable their greater use, the present research aimed to complex coriander and oregano EOs with beta-
189 CD, and characterize them using ATR-FTIR, Micro-Raman, DSC and TGA methodologies.
190 Antimicrobial activity assay of EOs were carried out against different bacteria and yeasts, and the
191 antioxidant activity and stability of free and complexed EOs were evaluated against high
192 temperatures. Additionally, a food application was made.

193

194 **2 Material and methods**

195 **2.1 Materials**

196 The main materials and reagents used: essential oil of *Coriandrum sativum* L., Apiaceae
197 (Steam distillation of the seed; Origin: Liechtenstein. Via Aroma, Porto Alegre, Brazil) and *Origanum*
198 *vulgare* (Steam distillation of the herb; Origin: Greece. Laszlo, Belo Horizonte, Brazil). Beta-
199 cyclodextrin (Sigma-Aldrich St. Louis, MO, USA).

200

201 **2.2 Characterization of coriander and oregano EOs**

202 The methodology used for the chemical characterization of EOs was based on Castro et al.
203 (2022) with modifications and was carried out using gas chromatography coupled to mass
204 spectrometry (GC-MS) (FOCUS GC - DSQ II equipment, Thermo Electron Corporation) equipped
205 with a DB-5MS column (5% phenyl/95% dimethylsiloxane stationary phase, 0.25 mm internal
206 diameter, 30 m long and 0.1 µm film of thickness). For the analysis, 1 µl of EO was injected in Split
207 mode (1:20), and the solvent used was hexane. The temperature of the injector and detector used was
208 250 °C and the oven temperature started at 40 °C and remained for 1 min. A gradient from 5 °C/min
209 until reaching 250 °C was adopted, at which it remained for 5 min. The interface temperature was
210 270 °C. Helium gas was used at a constant flow of 1.0 mL/min. The operation mode was by electron
211 impact at 70 eV.

212 The main compounds were characterized using retention time (RT) compared to the Kovats
213 retention rate (Skoog et al., 2006). The n-alkane standard was used to confirm the compounds
214 identified in the EOs, which were also confirmed by comparison with the literature (Adams, 2007).

215

216 **2.3 Complex formation**

217 The methodologies used to form the complex were cited by Miyoshi et al. (2022) with
218 modifications. The complexes were prepared by kneading and co-precipitation methods, and the

219 physical mixture was pre-established as a comparison standard in the analyzes carried out. The
220 proportion of EO and beta-CD in all methodologies was 1:1 (mol:mol), according to the main
221 component of each EO.

222 To prepare the physical mixture, in a glass mortar, the EO was added over the beta CD, which
223 was mixed manually. In the kneading methodology, a paste was formed with the EO and beta-CD by
224 gradually adding distilled water:ethanol (1:1) (v/v) and kneading with the aid one glass mortar and
225 pistil. A desiccator at room temperature was used to dry the complex. In the co-precipitation method,
226 beta-CD was solubilized at 70 °C and stirring in 20 mL of distilled water, and EO was solubilized in
227 3 mL of ethanol and added dropwise into the beta-CD solution. This system was kept under stirring
228 for 2 h on a magnetic stirrer. The complex was vacuum filtered using filter paper and left in a
229 desiccator for drying and subsequent storage. The complexes and physical mixtures were stored in a
230 hermetically sealed jar of glass protected from light.

231

232 **2.4 Determination of complexing efficiency (CE%)**

233 The amount of EO contained in the inclusion complexes (IC) was determined by the
234 complexing efficiency (CE%) based on the methodology of Castro et al. (2022), with modifications.
235 The spectral peaks were obtained using the UV-Vis spectrophotometer (VARIAN CARY 50 CONC
236 - Califórnia, USA). Initially, 1 mg of each EO was weighed and a full scan from 200 to 800 nm of
237 the EOs was performed to verify the appropriate wavelength for each sample. The absorbance
238 equivalent to 1 mg of pure EO was measured at the wavelength of each EO. Next, the same equivalent
239 amount of EO present in the physical mixture and in the IC were weighed, thus, 8.37 and 8.57 mg of
240 physical mixture and coriander and oregano EO complexes were weighed, respectively. To extract
241 the EO from the complex, ethanol was used in an amount of 1 mL, the samples were vortex
242 homogenized for 5 min, centrifuged at 4000 rpm and the absorbances measured. The blank used was
243 the solvent ethanol and the absorbance of beta-CD was discounted in all measurements. CE% was
244 determined by Equation: $CE\% = ((ABS_{EO-BETA-CD} - ABS_{BETA-CD}) / ABS_{EO}) \times 100$. Where, $ABS_{EO-BETA-CD}$
245 was the absorbance of the EO present in the physical mixture or in the IC, $ABS_{BETA-CD}$ was the
246 absorbance of beta-CD, and ABS_{EO} was the absorbance of free EO.

247

248 **2.5 Inclusion complexes characterization**

249 For the ATR-FTIR analysis, a Fourier transform infrared (FTIR) spectrometer (model Vertex
250 70v, Bruker, Germany) accessorized with attenuated total reflectance (ATR) was used, the spectral
251 region analyzed was from 400 to 4000 cm^{-1} , with a resolution of 4 cm^{-1} , and the results obtained were
252 the averages of the 128 readings that the device performs. For Micro-Raman spectra, the samples
253 were analyzed using the SENTERRA model spectrometer for Raman scattering (Bruker, Germany),

254 in which 20x approximation lenses and laser was used for excitation at 785 nm with 100 mW potency.
255 The resolution was 3 cm^{-1} , with a slit of $50 \times 100\text{ }\mu\text{m}$. The spectral range was from 70 to 3500 cm^{-1} ,
256 with an average of 30 combinations of 2 s integration time. The assays were performed in duplicate
257 (Miyoshi et al., 2022).

258 Thermal analyzes of beta-CD, the physical mixture and the IC were carried out using
259 differential scanning calorimetry (DSC) and thermogravimetry (TGA), measurements on the
260 equipment Perkin Elmer, modelo STA 6000 (Massachusetts, USA). The temperature range used was
261 50 to $550\text{ }^{\circ}\text{C}$, with a heating rate of $10\text{ }^{\circ}\text{C}/\text{min}$ and a nitrogen (N_2) flow of $50\text{ mL}/\text{min}$ (Miyoshi et
262 al., 2022).

263

264 **2.6 Antimicrobial activity**

265 The strains used to evaluate antimicrobial activity were *Escherichia coli* ATCC 25922,
266 *Salmonella enteritidis* ATCC 13076, *Pseudomonas aeruginosa* ATCC 27853 e 15442, *Bacillus*
267 *subtilis* ATCC 6633, *Staphylococcus aureus* ATCC 25923, *Candida albicans* ATCC 10231, *Candida*
268 *tropicalis* ATCC 28707 and *Candida parapsilosis* ATCC 22019. The microbial suspension was
269 standardized according to the turbidity equivalent to tube 0.5 on the McFarland scale and then diluted
270 1:10 in sterile saline. Free EOs, the physical mixture and ICs with beta-CD were evaluated.

271

272 **2.6.1 Broth Microdilution Method**

273 Suspensions containing 8 mg/mL of free EO were prepared and an equivalent amount of EO
274 was used for the IC, in other words, for the physical mixture and the complexes, solutions containing
275 66.9 mg/mL for the coriander EO and 68.6 mg/mL for the oregano EO were prepared. To solubilize
276 the EOs, 1% Tween 80 was used. The culture media for bacteria was Mueller Hinton broth (MHB)
277 and for yeast, RPMI-1640 with 0.05% phenol red supplemented with 10% glucose. A $100\text{ }\mu\text{L}$ volume
278 of culture medium was added to each well of a 96-well plate. Subsequently, $100\text{ }\mu\text{L}$ of the test solution
279 was added to the wells of the first column and then a serial dilution was carried out, resulting in
280 concentrations of 4000 to $15.63\text{ }\mu\text{g/ml}$. Then, $5\text{ }\mu\text{L}$ of the standard suspension of microorganisms
281 were added and incubated at $37 \pm 2\text{ }^{\circ}\text{C}$ during 48 h for bacteria and 72 h for *Candida* (Miyoshi et al.,
282 2022). In all assays, controls were performed on a culture medium, inoculum, EO, and their
283 complexes.

284 To determine the minimum bactericidal (MBC) and minimum fungicidal (MFC)
285 concentration, $10\text{ }\mu\text{L}$ of the culture medium was removed from the MIC and the wells above the MIC,
286 and this amount was plated on Müller-Hinton Agar (MHA) for bacteria and Sabouraud dextrose agar
287 for yeast. The plates were incubated at $37 \pm 2\text{ }^{\circ}\text{C}$ for 24 and 48 h for bacteria and yeast, respectively.

288 The lowest concentration of EO, physical mixture and IC in which there was no growth of
289 microorganisms was considered as MBC/MFC (Miyoshi et al., 2022).

290

291 **2.6.2 Agar dilution method**

292 The strains used to evaluate antimicrobial activity were *Escherichia coli* ATCC 25922,
293 *Staphylococcus aureus* ATCC 25923 e *Candida albicans* ATCC 10231. In sterile Petri dishes, EOs
294 and their IC were added and mixed with the agar (MHA and Sabouraud dextrose agar) at different
295 concentrations (250, 500, 1000 and 1500 µg/mL). The microorganisms were standardized using the
296 0.5 McFarland scale and diluted to a concentration of approximately 10⁴ CFU/mL. Then, 10 µL of
297 microorganisms were added to the plates and spread using a Drigalski spatula. The bacteria were
298 incubated at 37 °C for 24 h and the yeast was incubated at 37 °C for 48 h. The assays were performed
299 in triplicate with culture medium control and microorganism control (Castro et al., 2022).

300

301 **2.7 Phenolic compounds**

302 Using methanol as solvent, EOs were prepared at a concentration of 1 mg/mL. In 125 µL of
303 the solution containing the EO, 125 µL of the Folin-Ciocalteu 50% solution and 2250 µL of the
304 3,79 M sodium carbonate solution were added. The mixture was homogenized, left to rest for 30 min
305 and the reading was taken on a spectrophotometer at 725 nm. The blank was prepared by adding pure
306 solvent in place of the samples (Singleton & Rossi, 1965).

307

308 **2.8 Antioxidant activity**

309 the assay was carried out on a GENESYS 30 Thermo Fisher Scientific spectrophotometer
310 (Massachusetts, USA). To evaluate antioxidant activity, 1 mg of free EOs were weighed. The IC were
311 weighed with equivalent amounts of free EOs.

312

313 **2.8.1 DPPH radical scavenger activity**

314 The methodology used in this essay was based on Sousa et al. (2022). The stock solution of
315 DPPH 6.25x10⁻⁵ mols/L was adjusted to 0.700 at the absorbance of 517 nm (work solution). 25 µL
316 of the sample and 2 mL of the working solution were used. After preparing the samples, they were
317 left to rest for 30 min in the dark. Then the readings were taken at 517 nm by zeroing the device with
318 methanol. The result of DPPH radical scavenging activity was performed in triplicate and expressed
319 as the equivalent concentration of Trolox in µmol/mg of sample.

320

321

322 **2.8.2 ABTS radical scavenger activity**

323 According to the methodology of Sousa et al. (2022), the radical was obtained using 5 mL of
324 7,0 mmol/L ABTS stock solution with 88 µL of 140,0 mmol/L potassium persulfate solution, left to
325 rest for 12 to 16 h, in the dark, at room temperature. The solution of ABTS⁺ was adjusted to 0.700 at
326 the absorbance of 734 nm. It was used 30 µL of the sample and 3 mL of the ABTS⁺ solution and
327 kept in the dark for 6 min. The result of ABTS⁺ radical scavenging activity was expressed as the
328 equivalent concentration of Trolox in µgmol/mg of sample.

329

330 **2.7.4 Stability of the antioxidant activity of EOs**

331 The analysis was performed with EOs that demonstrated antioxidant activity at a temperature
332 of 25 °C. It was weighed 1 mg of EOs and the equivalent amount of EO in the complexes and placed
333 in screw-capped glass tubes. The temperatures tested were 80, 100, 120, 140 and 160 °C. After the
334 oven reached the desired temperature, the samples were placed and kept for 3 h. At the end, they were
335 cooled in an ice bath, 1 mL of methanol was added, vortexed for 5 min, centrifuged at 4000 rpm for
336 2 min and antioxidant activity was determined using the ABTS and DPPH methodologies (Miyoshi
337 et al., 2022).

338

339 **2.8 Application of EO in food**

340 To prepare the food product, the EO that obtained the best results was used, therefore, the EO
341 of oregano was used. Considering that the dehydrated oregano plant has been used in artisanal
342 cooking to make flavored butter, in this research, oregano EO was used to replace the dehydrated
343 product. The purpose of incorporating oregano EO is to improve oxidative stability and add
344 antimicrobial protection, as well as adding a pleasant aroma. It was added 1% of oregano to
345 commercial butter and for IC and physical mixture, the equivalent amount of EO was added. A sample
346 containing butter and beta-CD was also prepared to evaluate the effects of adding CD. The samples
347 were mixed for 10 min using a silicone spatula for total homogenization and subsequent analysis.

348

349 **2.8.1 Evaluation of the oxidative stability of products using the Rancimat method**

350 The Rancimat method was used to evaluate the oxidative stability index of the butters
351 containing oregano EO and its IC (Pérez-López et al., 2021). The assays were carried out using 3 g
352 of sample. The oxidation stability analyzes at 120 °C were determined using an apparatus Metrohm
353 893 Professional Biodiesel Rancimat, preheated to 120 °C with a maximum temperature variation of
354 1.6 °C and air flow of 20 L/h. To obtain the oxidation point, the second derivative method was used
355 to determine the point of greatest inclination of the conductivity curve.

356

357 **2.9 Statistical analysis**

358 Results were evaluated by using the analysis of variance (ANOVA) and averages compared
 359 by using Tukey test at 5% of significance level. Statistica® Software was used.

360

361 **3 Results and Discussion**

362 **3.1 Characterization of coriander and oregano EOs**

363 The chemical composition and quantification of EOs were performed by GC-MS and are
 364 presented in percentages in Table 1.

365

366 Table 1: Chemical composition of coriander and oregano EOs (%) and their
 367 respective retention times (RT).

Compound	Coriander RT (min)	%	Oregano RT (min)	%
Limonene	11,24	6,53	-	-
Geraniol acetate	21,19	2,90	-	-
Alpha-pinene	9,39	9,50	-	-
Ortho-cymene	11,08	5,57	-	-
Gamma-terpinene	12,12	4,97	-	-
Linalool	13,36	62,62	-	-
Camphor	14,81	5,40	-	-
Beta-cymene	-	-	11,1	11,24
Thymol	-	-	18,91	13,87
Carvacrol	-	-	19,16	72,08

368

369 The major compounds present in coriander EO were linalool, with approximately 62% of the
 370 total composition, followed by alpha-pinene and limonene, with approximately 9 and 6%,
 371 respectively. Kačániová et al. (2020) reported linalool as the main compound in their work with
 372 approximately 66% of the total composition, indicating consistency in the results obtained in this
 373 research.

374 The compounds identified in the oregano EO were beta-cymene, thymol and carvacrol, with
 375 the latter being the majority compound with approximately 72%. The results obtained are consistent
 376 with the literature (Khan et al., 2018; Lombrea et al., 2020).

377

378 **3.2 Complexation efficiency (CE%)**

379 To evaluate the CE%, a scan was carried out in which it was verified that the absorption
 380 wavelengths of the coriander EO were 208.5 nm and the oregano EO were 280 nm. In this way, the
 381 physical mixture and IC were analyzed at the same wavelengths as their respective EOs. The
 382 coriander EO presented an CE% of $78 \pm 1.3\%$ for the co-precipitation method and $58 \pm 1.9\%$ for the

383 kneading method. Raveau *et al* (Raveau et al., 2021) worked with coriander EO encapsulated with
 384 beta-CD through simple mixing and obtained CE% ranging from 63 to 81%.

385 The oregano EO showed better results for the encapsulation processes, and the two
 386 methodologies used showed little statistical difference and high CE% values, which were $98 \pm 0.4\%$
 387 and $97 \pm 0.4\%$ for precipitation and kneading, respectively. Gaur et al. (2018) encapsulated oregano
 388 EO and carvacrol with beta-CD using a similar method to that used in the present research and
 389 obtained an CE% of 80.9 and 85.9%, respectively, suggesting that the method used in the present
 390 study may be suitable for the formation of IC between CDs and EO.

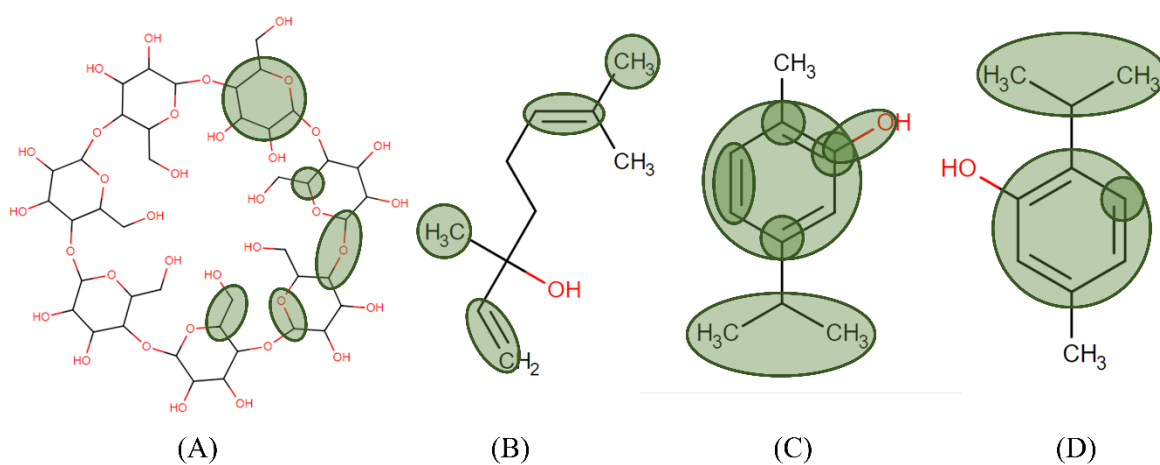
391

392 3.3 Characterization of ICs

393 3.3.1 Attenuated total reflection Fourier transform infrared (ATR-FTIR)

394 For guest molecules with low water solubility and high volatility, the most likely regions for
 395 molecular interactions are, for example, regions with double bonds and aromatic ring (Figure 1). The
 396 ATR-FTIR technique has been widely used to characterize IC with CDs. Based on previous studies,
 397 it was possible to assign the FTIR peaks to the main compounds of the different EOs, in addition to
 398 the FTIR of beta-CD (Kfouri et al., 2014; Li et al., 2010; Plati et al., 2021; Schulz et al., 2005;
 399 Shirirame et al., 2018; Siatis et al., 2005; Valderrama & Rojas De, 2017) (Table 2). In the present
 400 research, the physical mixture was used as a standard to observe the changes resulting from the
 401 possible encapsulation that occurred with the co-precipitation and kneading methodologies.

402



403

404 Figure 1: Probable bonds that underwent changes in vibrational mode after complexation. (A) beta-
 405 CD: glucose ring bonds; C-H bonds; C-O-C bonds; C-O bonds; C-C bonds. (B) Linalool: C=C
 406 bonds; C-H₃ bonds. (C) Carvacrol: aromatic ring bonds; C-H bonds; 1:2:4 substitution; C-O bonds;
 407 isopropyl methyl group; C=C bonds; C-H(CH₃) bonds. (D) Thymol: aromatic ring bonds; C-H
 408 bonds; isopropyl methyl group; C-H(CH₃) bonds.

409 Table 2: ATR-FTIR and Micro-Raman vibration modes of beta-CD and compounds present in EOs obtained experimentally and according to the
 410 literature (theoretical).

Sample	Experimental ATR-FTIR (cm ⁻¹)	Theoretical ATR-FTIR (cm ⁻¹)	Experimental Micro-Raman (cm ⁻¹)	Theoretical Micro-Raman (cm ⁻¹)	Vibration Mode	References
Beta-CD	574,7	579,0	476,5	478,0	Out-of-plane deformation of the glucose ring	(Li et al., 2010)
			500,0	497,0	Out-of-plane bending (O–H)	(Li et al., 2010)
			571,0	583,0	Out-of-plane bending (O–H)	(Li et al., 2010)
			651,0	649,0	Out-of-plane bending (O–H)	(Li et al., 2010)
	705,9	707,0	709,5	711,0	In-plane deformation of glucose ring	(Li et al., 2010)
			753,5	754,0	In-plane deformation of glucose ring	(Li et al., 2010)
	854,4	859,0	853,0	851,0	Breath of glucose ring	(Li et al., 2010)
			928,0	929,0	Breath of glucose ring	(Li et al., 2010)
	945,0	944,0	948,5	948,0	Symmetrical stretching (C–O–C)	(Li et al., 2010)
	999,0	996,0			Symmetrical stretching (C–O–C)	(Li et al., 2010)
	1020,2	1026,0	1047,5	1046,0	Stretching (C–O)	(Li et al., 2010)
	1076,1	1080,0	1083,5	1085,0	Stretching (C–O)	(Li et al., 2010)
			1127,0	1127,0	Stretching (C–C)	(Li et al., 2010)
	1153,3	1159,0			Symmetrical stretching (C–O–C)	(Li et al., 2010)
	1251,6	1246,0	1250,5	1252,0	Scissoring (C–H)	(Li et al., 2010)
	1297,9	1300,0			Scissoring (C–H)	(Li et al., 2010)
	1334,5	1335,0	1325,0/1337,0	1333,0	Scissoring (C–H)	(Li et al., 2010)
	1365,4	1368,0	1388,0	1388,0	Scissoring (C–H)	(Li et al., 2010)
	1413,6	1418,0	1409,8	1407,0	Scissoring (O–H)	(Li et al., 2010)
			1452,0	1450,0	Scissoring (C–H ₂)	(Li et al., 2010)
	1643,1	1647,0			Stretching (O–H)	(Li et al., 2010)

411 * Continue.

412

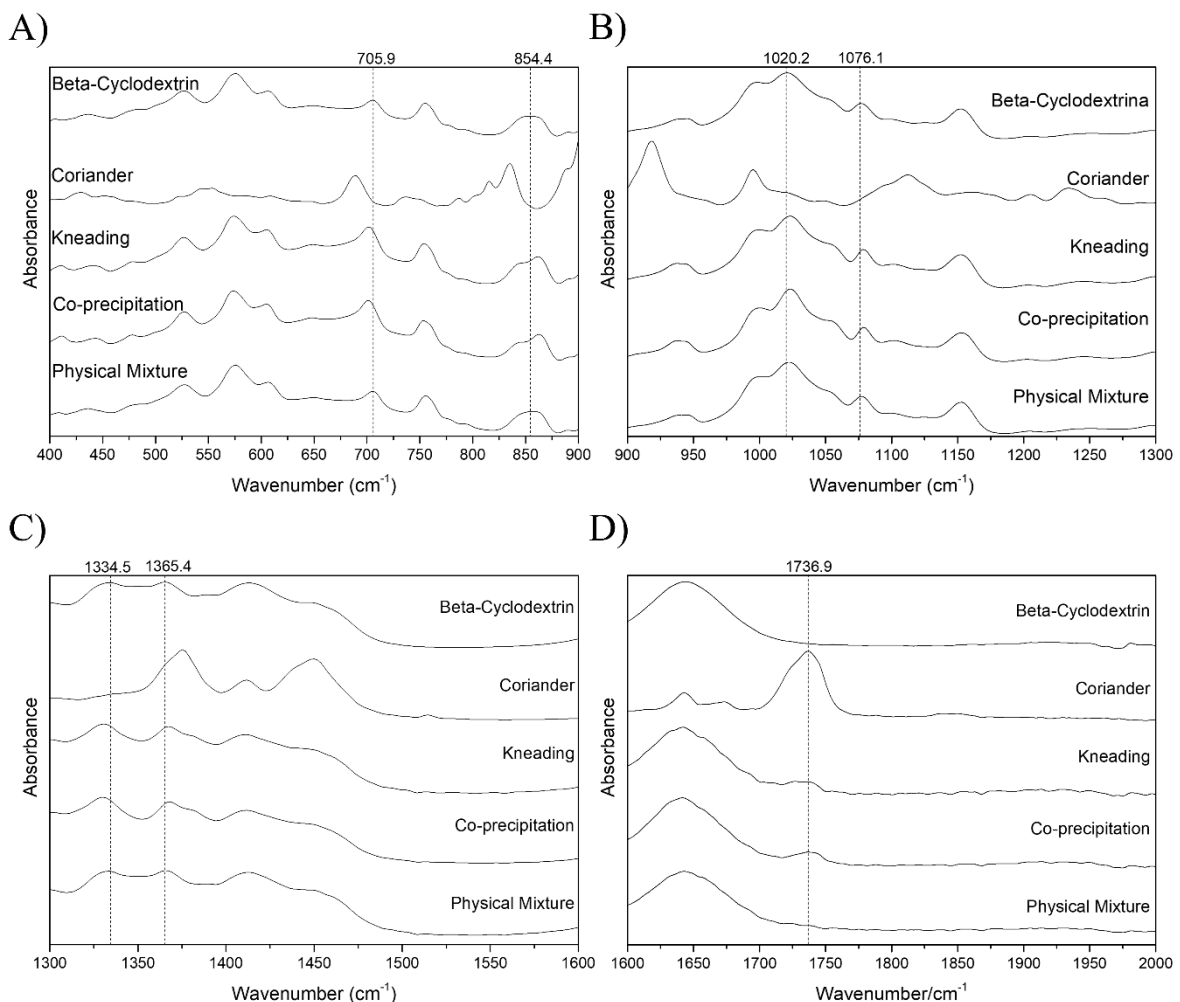
413

414 Table 2: ATR-FTIR and Micro-Raman vibration modes of beta-CD and compounds present in EOs obtained experimentally and according to the
 415 literature (theoretical).*

Sample	Experimental ATR-FTIR (cm ⁻¹)	Theoretical ATR-FTIR (cm ⁻¹)	Experimental Micro-Raman (cm ⁻¹)	Theoretical Micro-Raman (cm ⁻¹)	Vibration Mode	References
Coriander			1372,0	1378,0	Bending (C–H ₃) – linalool	(Jentzsch et al., 2015), (Hanif et al., 2017; Kfouri et al., 2014), (Shrirame et al., 2018)
	1643,1	1644,0	1671,0	1671,0	Stretching (C=C) – linalool	
	1736,9	1742,0			Stretching (C=O)	
			739,0	740,0	Breath of glucose ring – thymol	(Siatis et al., 2005)
			759,5	760,0	Breath of glucose ring – carvacrol	(Siatis et al., 2005)
			885,5	880,0	Out-of-plane bending (C–H) – carvacrol/thymol	(Siatis et al., 2005)
	810,0	811,0	1058,5	1060,0	Out-of-plane bending (C–H) aromatic ring – carvacrol/thymol	(Schulz et al., 2005; Siatis et al., 2005), (Plati et al., 2021)
	937,3	939,0			Bending (C–H) of the aromatic ring – carvacrol	
	995,2	995,0			1:2:4 substitution – carvacrol	(Valderrama & Rojas De, 2017)
	1251,6	1254,0	1180,0-1261,5	1180,0-1260,0	Phenyl core stretching – carvacrol/thymol Stretching (C–O–C) – carvacrol	(Siatis et al., 2005) (Plati et al., 2021)
Oregano	1361,5	1362,0			Isopropyl group – carvacrol/thymol	(Valderrama & Rojas De, 2017)
			1379,5	1380,0	Asymmetric isopropyl methyl group – carvacrol/thymol	(Siatis et al., 2005)
			1445,0-1460,0	1440,0-1460,0	Symmetric isopropyl methyl group – carvacrol/thymol	(Siatis et al., 2005)
	1419,4	1424,0			Stretching (C=C) aromatic ring – carvacrol	(Plati et al., 2021)
	1502,3-1521,6	1513,0-1520,0			C–H(CH ₃) – carvacrol/thymol	(Valderrama & Rojas De, 2017)
			1622,0	1623,0	Stretching C=C conjugate – carvacrol/thymol	(Siatis et al., 2005)

The ATR-FTIR spectra referring to coriander EO, beta-CD, physical mixing, co-precipitation and kneading are shown in Figure 2. In Figure 2A, for coriander EO, regions of peak shifts were observed in both the beta-CD bonds and the bonds of the major compound linalool. The beta-CD presented a peak at 705.9 cm^{-1} corresponding to the in-plane deformation glucose ring (Li et al., 2010) (Table 2), which was shifted to 702.0 cm^{-1} for the IC while the physical mixture remained in the same position. It is possible to suggest that in the band at 854.4 cm^{-1} , referring to the breath of glucose ring (Li et al., 2010), two peaks of equivalent intensities overlap and that due to the complexation process, these overlapping peaks presented different intensities.

10



11

Figure 2: ATR-FTIR spectrum for coriander EO, beta-CD, physical mixture and IC formed from co-precipitation and kneading methodologies. (A) Magnification in the region of $400\text{-}900\text{ cm}^{-1}$. (B) Magnification in the region of $900\text{-}1300\text{ cm}^{-1}$. (C) Magnification of $1300\text{-}1600\text{ cm}^{-1}$. (D) Magnification in the region of $1600\text{-}1800\text{ cm}^{-1}$.

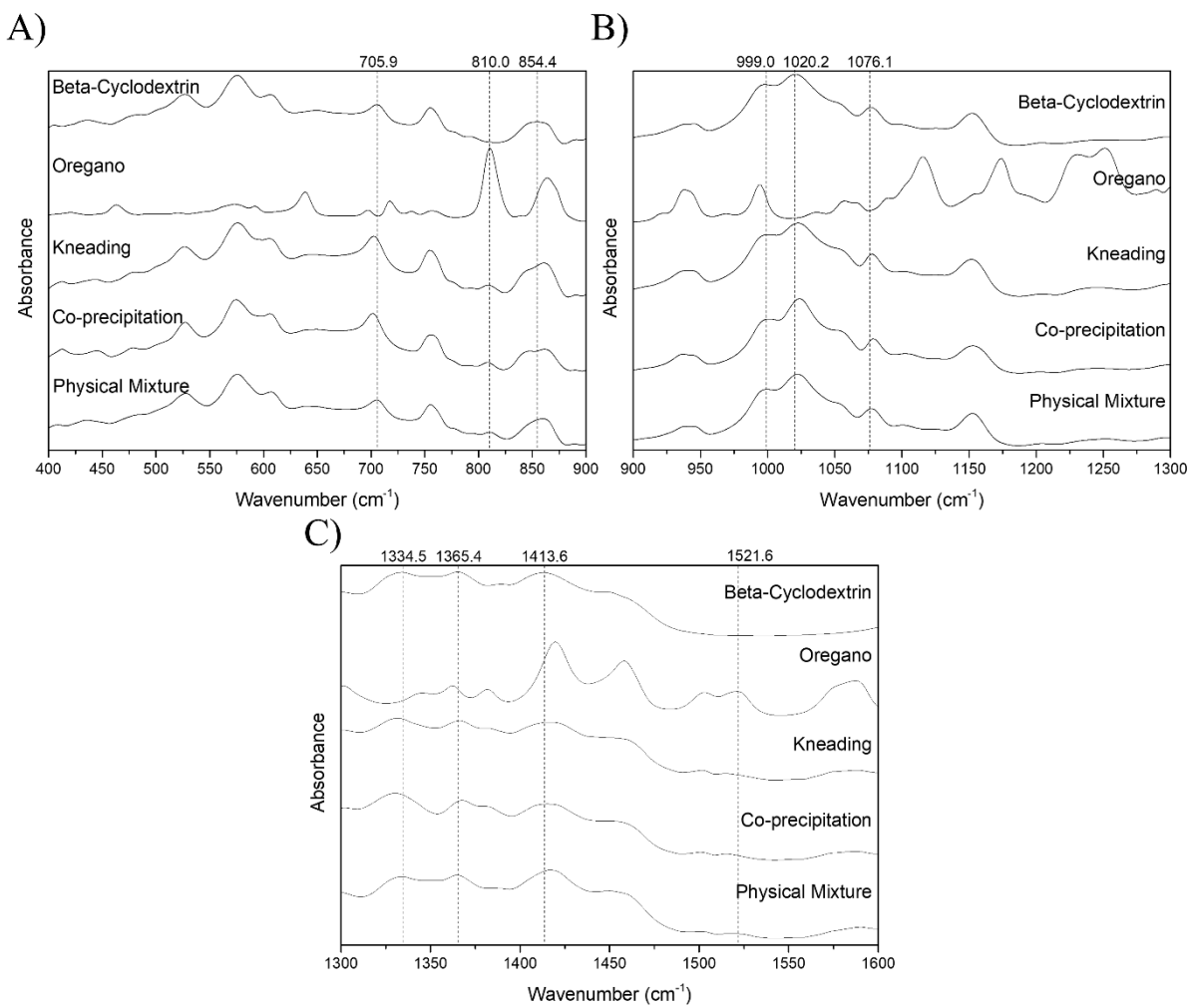
16

1 In Figure 2B, two regions of peak shifts were observed in the beta CD spectrum referring
2 to the stretching C–O (Li et al., 2010) (Table 2). The wavenumber at 1020.2 cm⁻¹ was shifted
3 to 1022.1 cm⁻¹ in kneading and physical mixture, while for co-precipitation the shift was to
4 1024.0 cm⁻¹. Al-Shar'i & Obaidat (2018) showed evidence the complexation between beta-CD
5 and the compounds linalool and carvacrol, and stated that the peak at 1020.2 cm⁻¹ indicates the
6 C–O stretch bonds of beta-CD. At 1076.1 cm⁻¹, all samples showed the same shift for the
7 wavenumber 1078.0 cm⁻¹.

8 The scissor C–H vibrational mode of beta-CD (Table 2) was observed in Figure 2C,
9 with peaks at 1334.5 and 1365.4 cm⁻¹. In both complexes it was verified the displacements were
10 1330.7 and 1367.3 cm⁻¹, respectively. At 1334.5 cm⁻¹, the physical mixture underwent a small
11 shift to 1332.6 cm⁻¹, in which it remained unchanged at the wavelength of 1365.4 cm⁻¹. Similar
12 displacements were observed by Kfouri et al. (2014) in the scissor C–H vibration modes of
13 beta-CD and linalool.

14 In Figure 2D, a peak at 1736.9 cm⁻¹ was observed in the spectrum of coriander EO,
15 corresponding to the C=O (Li et al., 2010) stretch which is not present in the spectrum of beta-
16 CD and the physical mixture. For the IC there was a small shift to 1737.6 cm⁻¹ in kneading and
17 1735.7 cm⁻¹ in co-precipitation. Therefore, it is possible to suggest that interactions between
18 the guest molecule and host affected the movements of this bond.

19 In Figure 3 shows the ATR-FTIR spectra of oregano EO, beta-CD and ICs. For beta-CD,
20 similar shifts were observed in the assay with coriander EO. In Figure 3A, the peak at 705.9
21 cm⁻¹ shifted to 702.0 cm⁻¹ in both ICs, and the physical mixture remained unchanged, which
22 suggests that the kneading and co-precipitation methodologies are effective in the complexation
23 of oregano EO with beta CD. Still in Figure 3A, the oregano EO presented a peak at 810.0 cm⁻¹,
24 corresponding to the out-of-plane CH bending of the aromatic ring of carvacrol (Siatis et al.,
25 2005), which moved to 808.1 cm⁻¹ in both ICs, the physical mixture remains at the same
26 wavelength as the EO. The changes observed in the aromatic ring of carvacrol were a great
27 indication of the process of formation of the ICs since the beta-CD cavity has a great affinity
28 with lipophilic compounds, such as aromatic rings. The beta-CD band, in which the peak at
29 854.0 cm⁻¹ is present, had its spectrum altered when EO was added. This region corresponds to
30 the breathing movement of the beta-CD glucose ring (Table 2) and is of great interest, as it
31 strongly suggests the presence of compounds within the beta-CD cavity, preventing this
32 movement, which was reflected in the spectrum.



1
2 Figure 3: ATR-FTIR spectrum for oregano EO, beta-CD, physical mixture and ICs formed from
3 co-precipitation and kneading methodologies. (A) Magnification in the region of 400-900 cm⁻¹.
4 (B) Magnification in the region of 900-1300 cm⁻¹. (C) Magnification of 1300-1600 cm⁻¹.

5
6 In Figure 3B, the peak at 999.0 cm⁻¹ of beta-CD was shifted to 1000.9 cm⁻¹ in both ICs
7 and the physical mixture remained unchanged. At 1020.2 cm⁻¹, both kneading and physical
8 mixing shifted to 1022.1 cm⁻¹, while co-precipitation had a larger shift to 1024.0 cm⁻¹. At
9 1076.1 cm⁻¹ the physical mixture and both ICs moved to 1078.0 cm⁻¹. These modifications
10 indicate that even in very simple preparations such as physical mixtures, the encapsulation
11 process can occur, however, these bonds are not strong enough to maintain the formed complex.

12 In Figure 3C, the peak at 1334.5 cm⁻¹ shifted to 1330.7 cm⁻¹ in both ICs. Beta-CD
13 exhibited a peak at 1365.4 cm⁻¹, while oregano EO showed a peak at 1361.5 cm⁻¹, characteristic
14 of the isopropyl group present in carvacrol and thymol (Table 2). A shift of 1367.3 cm⁻¹ was
15 observed only for the complex formed by co-precipitation. The physical mixture did not shift.
16 Peaks were observed at 1413.6 and 1419.4 cm⁻¹ for beta-CD and oregano EO, respectively.

1 Plati et al. (2021) describe that the peak present in the EO spectrum is characteristic of the C–
2 C stretching of the aromatic ring of carvacrol (Table 2). In both ICs, the peak moved to 1415.5
3 cm⁻¹ and for the physical mixture, the peak was observed at 1417.5 cm⁻¹. The last peak in Figure
4 3C is characterized by the vibration mode that occurs in the C–H(CH3) portion of carvacrol
5 and thymol mentioned by Valderrama & Rojas De, 2017) (Table 2), which appeared in the
6 spectrum at 1521.6 cm⁻¹. The changes found in the wavenumbers of the complexes are strong
7 indications of the formation of ICs between oregano EO and beta-CD.

8 According to Sun et al. (2022), who complexed carvacrol with hydroxypropyl-beta-CD,
9 notable peaks in carvacrol that disappeared after complexation could characterize the formation
10 of the EO-beta-CD ICs. Trindade et al. (2019) also described changes in displacement and
11 intensity in carvacrol-beta-CD ICs.

12

13 3.3.2 Micro Raman

14 The Micro-Raman technique is complementary to the ATR-FTIR technique. Based on
15 previous studies, it was possible to assign the Raman peaks to the main compounds of the
16 different EOs and beta-CD (Jentzsch et al., 2015; Li et al., 2010; Schulz et al., 2005) (Table 2).
17 The possible regions affected by the encapsulation process are illustrated in Figure 1. The
18 physical mixture was again used as a standard so that it was possible to evaluate possible
19 changes in molecular vibration after the encapsulation process.

20 Figure 4 shows the Micro-Raman spectra of coriander EO, beta-CD, and ICs. In Figure
21 4A, the peak at 476.5 cm⁻¹, characteristic of the out-of-plane deformation of the beta-CD
22 glucose ring (Table 2), has shifted to 481.5 cm⁻¹ in both ICs. CDs are formed by several glucose
23 units, therefore, changes in the bonds of the beta-CD glucose ring are a strong indication that
24 the microencapsulation process has occurred, corroborating the results obtained in the
25 ATR-FTIR spectrum. The physical mixture spectrum remained unchanged. The out-of-plane
26 O–H bending-type vibrations of beta-CD at 571.0 and 651.0 cm⁻¹ (Table 2) were shifted to
27 575.0 and 647.0 cm⁻¹, respectively, for both kneading and co-precipitation methods. The
28 physical mixture remained as beta-CD at 571.0 cm⁻¹, however, at 651.0 cm⁻¹ it moved to
29 649 cm⁻¹.

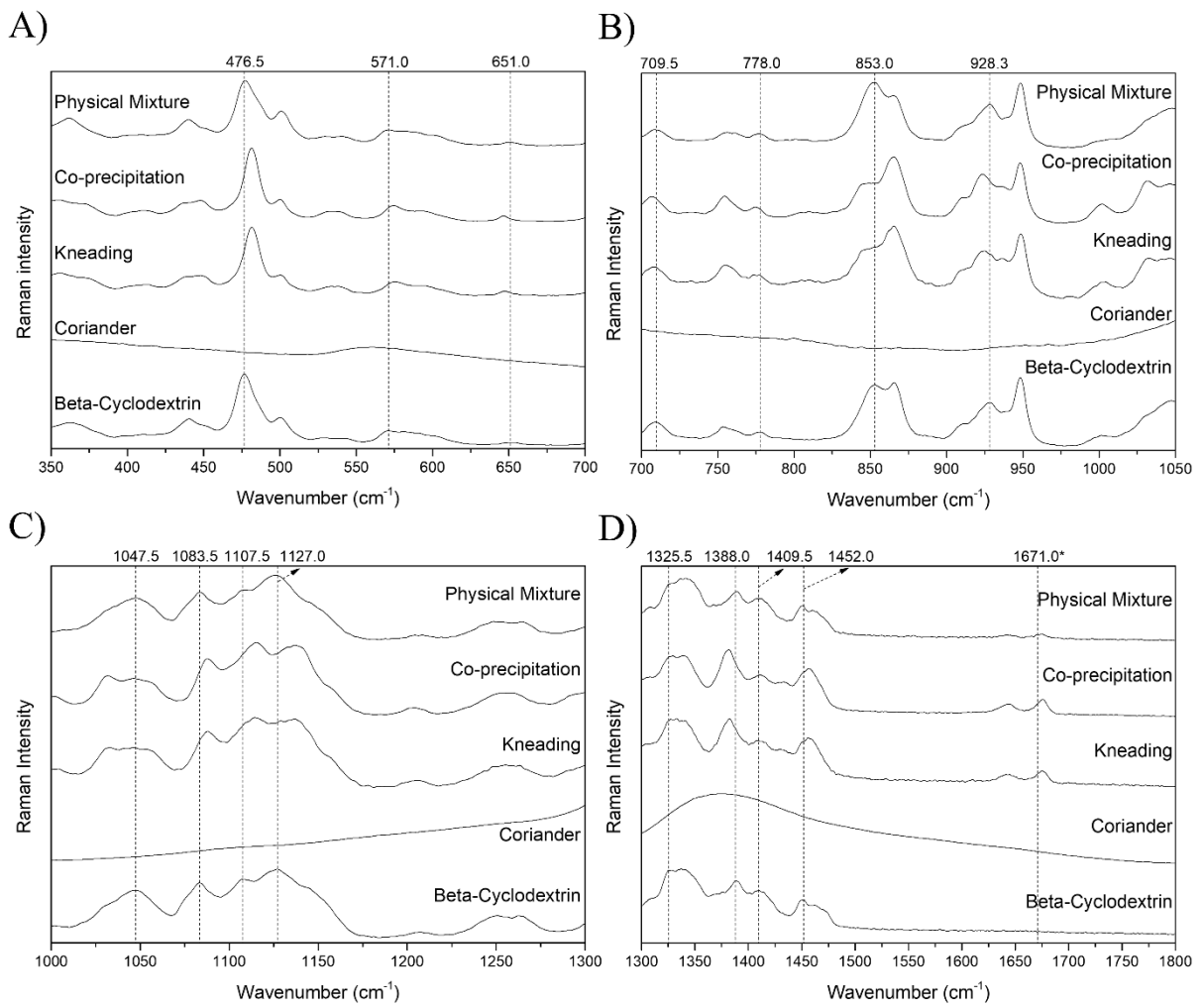


Figure 4: Micro-Raman spectrum for coriander EO, beta-CD, physical mixture, and IC formed from co-precipitation and kneading methodologies. (A) Magnification in the region of $350\text{-}700\text{ cm}^{-1}$. (B) Magnification in the region of $700\text{-}1050\text{ cm}^{-1}$. (C) Magnification of $1000\text{-}1300\text{ cm}^{-1}$. (D) Magnification of $1300\text{-}1800\text{ cm}^{-1}$. * Value obtained from literature: Hanif et al. (2017).

7

In Figure 4B, the peaks at 709.5 and 778.0 cm^{-1} , corresponding to the in-plane deformation of the beta-CD glucose ring (Table 2), have also shifted. At 709.0 cm^{-1} , kneading and physical mixture shifted to 708.0 cm^{-1} and precipitation shifted to 706.5 cm^{-1} . For the peak at 778.0 cm^{-1} , the displacements were 773.5 , 774.5 , and 777.0 cm^{-1} for kneading, co-precipitation, and physical mixture, respectively. Again, changes in the glucose ring of beta-CD are a strong indication that a molecule may be inside the CD cavity (Figure 4B), corroborating the results found in ART-FTIR. The band at 853.0 cm^{-1} of the ICs was disfavored about the beta-CD spectrum and the peak was shifted to 848.5 cm^{-1} . This region is characteristic of the breathing vibration of the beta-CD glucose ring and the same vibration was found at

1 928.3 cm⁻¹ (Table 2). The peak at 928.3 cm⁻¹ was shifted to 925.0 and 923.5 cm⁻¹ in kneading
 2 and co-precipitation, respectively. Once again, it was possible to emphasize that the inclusion
 3 of the guest in the beta-CD cavity may cause a disadvantage of this mode of vibration, indicating
 4 that the formation of the ICs may have occurred.

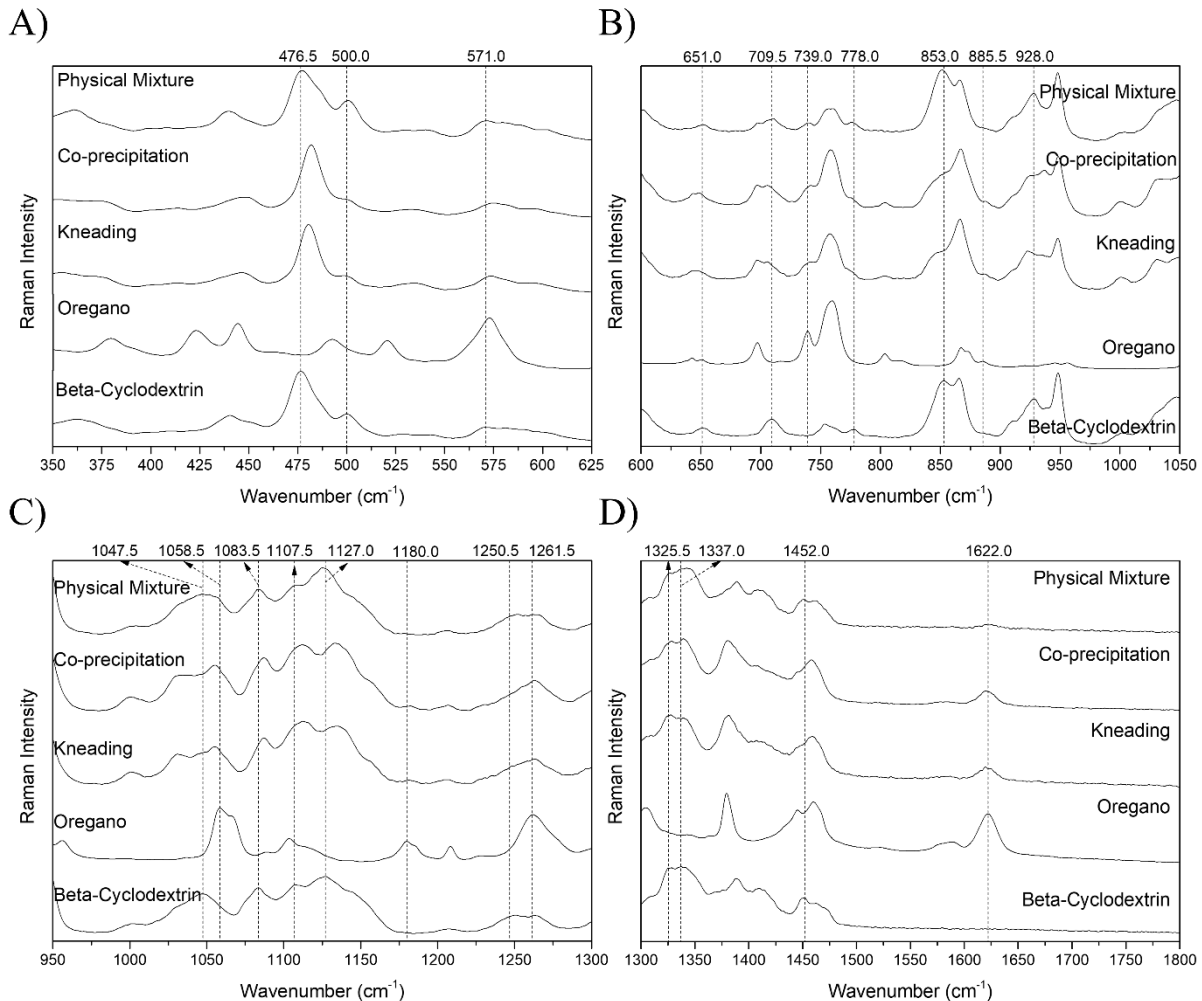
5 In Figure 4C, the region of the spectrum that goes from 1047.5 to 1127.0 cm⁻¹ refers to
 6 the C–O and C–C stretches of beta-CD (Table 2), and throughout the region, it was possible to
 7 observe different changes. The peak at 1047.5 cm⁻¹ of beta-CD was disfavored and moved to
 8 1032.5 cm⁻¹ in both ICs. At 1083.5, 1107.5 and 1127.0 cm⁻¹ the spectra of the ICs shifted to
 9 1088.0, 1115.0, and 1137.0 cm⁻¹, respectively. The physical mixture remained unchanged about
 10 the beta CD, except for at 1107.5 cm⁻¹, where it shifted to 1109.0 cm⁻¹. (Castro et al., 2022)
 11 complexed the *Cymbopogon martini* EO with beta-CD, which contains linalool in its
 12 composition, and observed displacements related to the C–C stretching of beta-CD, suggesting
 13 the formation of the ICs.

14 In Figure 4D, the peaks at 1325.5 and 1388.0 cm⁻¹ are also attributed to the previously
 15 mentioned vibration mode. The first peak shifted to 1327.5 cm⁻¹ in kneading, 1329.5 cm⁻¹ in
 16 co-precipitation, and 1328.0 cm⁻¹ in physical mixture. The next peak was more intense due to
 17 the complexation process, moving to 1382.5 cm⁻¹ in the ICs and to 1389.0 cm⁻¹ in the physical
 18 mixture. In this region, a peak was also identified at 1372.0 cm⁻¹ corresponding to the C–H₃
 19 flexion of linalool (Table 2) present in the EO. The peak at 1409.5 cm⁻¹, corresponding to the
 20 O–H scissor mode of beta-CD (Table 2), shifted to 1408.0 cm⁻¹ in kneading and 1411.0 cm⁻¹ in
 21 co-precipitation and physical mixture. The peak at 1452 cm⁻¹, corresponding to the C–H₂ scissor
 22 vibration mode of beta-CD (Table 2), was shifted to 1456.5 cm⁻¹ in both ICs. The physical
 23 mixture had an inverse shift to 1450.5 cm⁻¹.

24 In the spectrum of beta-CD and coriander EO, no peaks were observed in the region of
 25 1600 to 1700 cm⁻¹, however, when analyzing the spectra of the ICs, peaks were observed in this
 26 region, which require different studies to justify them. (Hanif et al., 2017), in their work,
 27 described a linalool peak at 1671.0 cm⁻¹ referring to stretching C=C (Table 2), being another
 28 suggestion that the formation of the complex favored the vibration modes of coriander EO.

29 The Micro-Raman spectrum for oregano EO is shown in Figure 5. In Figure 5A, at 476.5
 30 cm⁻¹, the kneading shifted to 480.5 cm⁻¹ and the co-precipitation to 482.0 cm⁻¹. The O–H out-
 31 of-plane bending vibrational mode of beta-CD at 500.0 cm⁻¹ (Table 2) was undermined in the
 32 signal strength, in kneading there was a small shift to 498.5 cm⁻¹, and in co-precipitation, it was
 33 not possible to identify the peak shift. In all vibration modes in Figure 5A, the physical mixture
 34 remained unchanged. The beta-CD and physical mixture peak appears at 571.0 cm⁻¹, the

- 1 oregano EO and kneading peak at 573.0 cm^{-1} , and only for co-precipitation was a shift observed
 2 to 575.0 cm^{-1} .
 3



4
 5 Figure 5: Micro-Raman spectrum for oregano EO, beta-CD, physical mixture, and IC formed
 6 from co-precipitation and kneading methodologies. (A) Magnification in the region of
 7 $350\text{-}625\text{ cm}^{-1}$. (B) Magnification in the region of $600\text{-}1050\text{ cm}^{-1}$. (C) Magnification of
 8 $950\text{-}1300\text{ cm}^{-1}$. (D) Magnification of $1300\text{-}1800\text{ cm}^{-1}$.

9
 10 In Figure 5B, the oregano EO peak appears at the same wavelength as beta-CD, at
 11 651.0 cm^{-1} and, for both ICs, a shift to 648.5 cm^{-1} was observed. The physical mixture remained
 12 unchanged. The peak at 709.5 cm^{-1} , corresponding to the in-plane deformation of the beta-CD
 13 glucose ring (Table 2), shifted to 705.5 , 706.0 , and 710.5 cm^{-1} for the kneading, in the co-
 14 precipitation and physical mixture, respectively. At the peak at 739.0 cm^{-1} , corresponding to
 15 the breathing vibration of the thymol aromatic ring (Table 2), there was a disfavoring of the
 16 peak and a shift to 741.0 and 742.0 cm^{-1} in kneading and co-precipitation, respectively.

The changes in the peaks referring to the aromatic rings of the compounds present in the oregano EO were a strong indication of complexation, since this part of the molecule is inside the CD cavity, preventing its proper movement and repercussion in the Micro-Raman spectrum. Also, in Figure 5B, the peak at 778 cm^{-1} is related to the deformation in the plane of the β -CD glucose ring. This peak was disfavored in the ICs and, only in co-precipitation, it was possible to observe a shift to 775.5 cm^{-1} . In the physical mixture, the peak characteristics remained as beta-CD, however, there was a small shift to 776 cm^{-1} . The changes observed in the physical mixture may indicate some interaction between the EO and CD, however, thermal tests showed that this interaction does not produce protection and stability effects for the compounds present in the EOs. The vibrations corresponding to the breathing of the beta-CD glucose ring (Table 2) at 853.0 cm^{-1} suffered disfavor at the peak and at 928.0 cm^{-1} a shift in kneading to 923.0 cm^{-1} and in co-precipitation to 926.0 cm^{-1} was observed. The physical mix did not change. The change in this vibrational mode may indicate that the guest was included in the beta-CD cavity, influencing the vibration of this functional group. These results also corroborate the results found in ATR-FTIR. In the spectrum of oregano EO, a peak was noted at 885.5 cm^{-1} , referring to the out-of-plane C–H bending, which could be from both carvacrol and thymol (Table 2). This peak moved to 887.0 cm^{-1} in both ICs and there was no change in the physical mixture.

In Figure 5C, numerous changes in the kneading and co-precipitation spectra are observed, strongly indicating that ICs were formed. At 1047.5 cm^{-1} , shifts and the appearance of a new peak were observed in both ICs, which may be related to the EO band at 1058.5 cm^{-1} , corresponding to the out-of-plane C–H bending of the carvacrol aromatic ring (Table 2). For kneading, the observed peaks appeared at 1031.0 and 1055.5 cm^{-1} , and for co-precipitation, at 1034.5 and 1055.0 cm^{-1} . At 1083 cm^{-1} , both ICs moved to 1087.0 cm^{-1} , while the physical mixture remained unchanged. The peaks at 1107.5 and 1127.0 cm^{-1} shifted in both ICs to 1112.0 and 1133.8 cm^{-1} , respectively. Only at 1127.0 cm^{-1} , the physical mixture showed a small shift to 1125.0 cm^{-1} . For carvacrol and thymol, a peak at 1180.0 cm^{-1} was reported, corresponding to stretching of the phenyl nucleus (Table 2), which shifted for the kneading and co-precipitation to 1181.5 and 1182.0 cm^{-1} , respectively.

The band that represents the C–H scissor vibration mode of beta-CD appeared in the region of 1250.5 to 1262.5 cm^{-1} (Table 2). In the same region, at 1261.5 cm^{-1} , the oregano EO exhibited a peak characteristic of stretching of the phenyl nucleus of carvacrol or thymol (Table 2). For both ICs, a disfavor at 1250.5 cm^{-1} and a shift to 1263.0 cm^{-1} were observed, these changes in the EO spectrum are strong indications of complexation (Figure 5C).

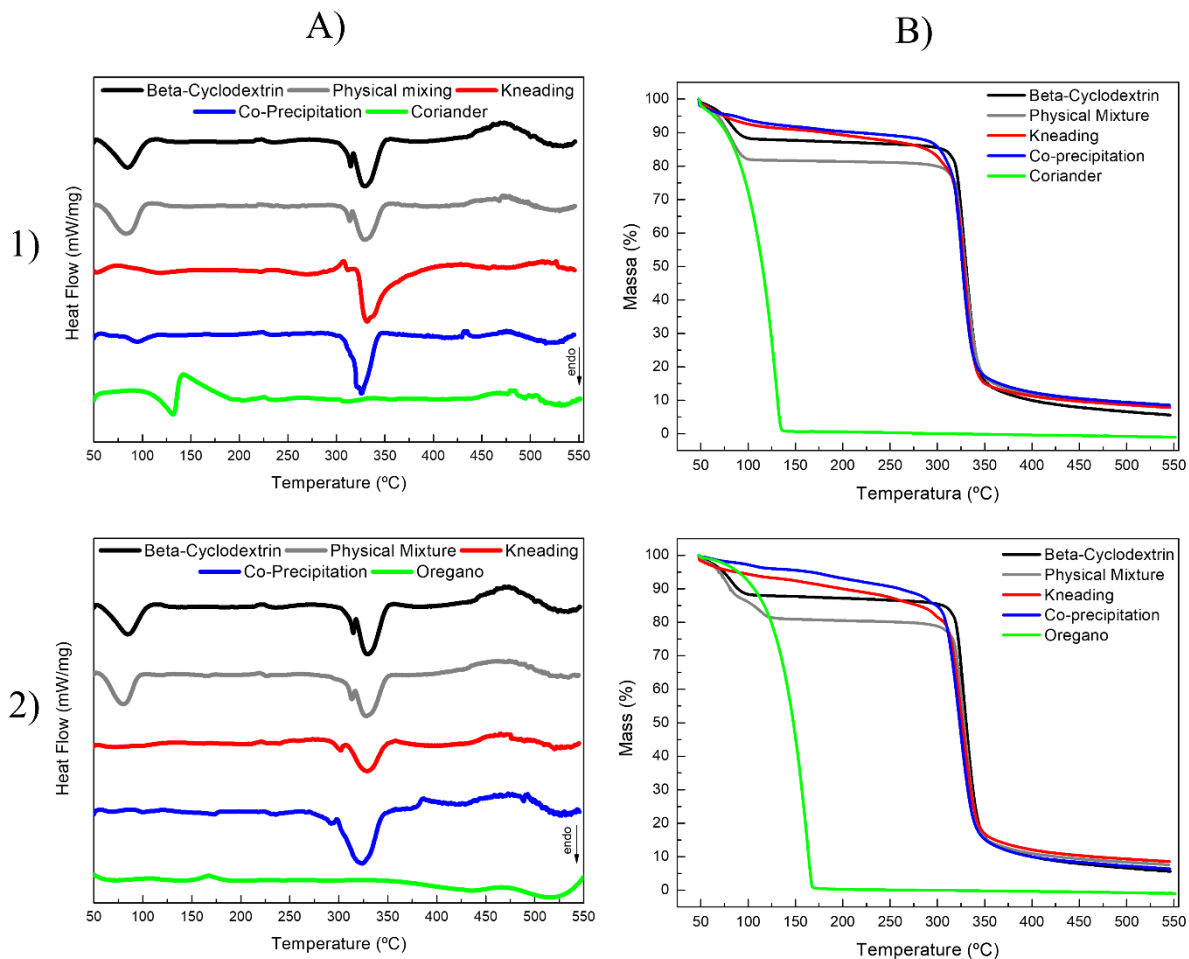
In the region from 1325.5 to 1337.0 cm⁻¹, the band corresponding to the CH scissor vibration of the beta-CD molecule (Table 2), different modifications occurred for the ICs and physical mixture. During kneading, there was favoring and shifts to 1328.0 cm⁻¹ and 1339.0 cm⁻¹. In co-precipitation, the same displacements were observed, however, there was a disadvantage at the beginning of the peak. For the physical mixture, the displacements were 1326.5 and 1342.0 cm⁻¹ (Figure 5D). Still, in Figure 5D, beta-CD exhibited a peak at 1452.0 cm⁻¹, referring to the C–H₂ scissor vibration mode, while oregano EO, the symmetric vibration mode of the isopropyl methyl group of carvacrol and thymol of 1445.0 to 1460.0 cm⁻¹. Both ICs suffered disfavor in this region and a peak shift to 1458.0 cm⁻¹. The physical mixture showed a junction of EO and beta-CD peaks. The peak at 1622.0 cm⁻¹ is related to the conjugated C=C stretching of carvacrol (Table 2) and moved to 1620 cm⁻¹ in the ICs and physical mixture, however in the physical mixture the signal is less intense, indicating that the complexation favored the carvacrol signal when compared to the physical mixture.

(Dai et al., 2022), when observing displacements, changes in conformations, and intensities in Raman peaks, suggested the encapsulation of thymol with beta-CD. In this research, different regions of carvacrol and thymol changed with the complexation process, suggesting that inclusion in the beta-CD cavity occurred with these compounds.

18

19 **3.3.3 Differential scanning calorimetry (DSC) and thermogravimetry (TGA)**

20 In DSC, beta-CD showed three endothermic events. The first event ranges from 50 to 21 113 °C and is characteristic of beta-CD dehydration. The second and third events are subsequent 22 and occur from 270 to 317 °C and 317 to 355 °C, these events are related to the process of 23 molecular decomposition and consequent removal of carbonaceous material (Miyoshi et al., 24 2022; Rodrigues et al., 2017). The physical mixture of the two EOs presented DSC curves 25 similar to beta-CD with differences in the positions of the endothermic peaks and no 26 characteristic EO events (Figure 6A). Considering that the TGA analyses complement the data 27 obtained in the DSC, the results referring to the complexes are presented below together with 28 the TGA data.



1
2 Figure 6: (A) DSC and (B) TGA of the EOs of (1) coriander and (2) oregano, the physical
3 mixture, and the ICs formed by the co-precipitation and kneading methodologies.
4

5 In the TGA analyses, the events occurring in the DSC were considered to determine the
6 mass loss (Δm) of the EOs, beta-CD, the physical mixture, and the ICs (Figure 6B). For
7 beta-CD, in the first endothermic event, Δm was 12%. This loss is associated with the surface
8 and internal water of beta-CD through the dehydration process (Abarca et al., 2016). From 113
9 to 270 °C, Δm of beta-CD was only 2%. In the second and third events (270 to 317 °C), Δm was
10 72%. At 550 °C, the final mass of beta-CD was 5% of the initial mass.

11 For the coriander EO, the endothermic peak was observed at 131 °C, corresponding to
12 its boiling point (Figura 6A1). In kneading, where should be the first endothermic event,
13 corresponding to the dehydration of beta-CD, an exothermic event occurred, which may be
14 related to the replacement of the water molecule by the EO. The second endothermic event also
15 becomes exothermic with a peak at 307 °C. At 317 °C the third endothermic event began,
16 peaking at 331 °C. For co-precipitation, the dehydration peak of beta-CD moved to 94 °C, being

1 a less evident peak than in beta-CD and in the physical mixture. The second event did not occur,
2 and the third event began at 287 °C, with an endothermic peak at 325 °C.

3 In the TGA analysis of coriander EO, it had a Δm of approximately 99% at 141 °C. The
4 physical mixture, in the first endothermic event, had a Δm of 18%. Between temperatures of
5 109 to 294 °C, Δm was approximately 2%. In the second and third endothermic event, Δm was
6 64%; and at 550 °C the physical mixture presented 8% of the initial mass. In kneading, from 50
7 to 117.5 °C, Δm was 8%, and from the end of the first event until the beginning of the second,
8 Δm was 6%. Using beta-CD degradation events as a basis, for coriander EO the Δm was 72%,
9 ending with a total Δm of 92%. In co-precipitation, Δm was 7% in the first event and 5% until
10 the beginning of the second event. The Δm of the degradation event was 70%. At the end of the
11 analysis, the total Δm was 91% (Figure 6B1).

12 DSC and TGA results for coriander EO suggested complexation by kneading and co-
13 precipitation methods. As for the physical mixture, it was observed that its behavior was similar
14 to beta-CD, however, due to the presence of EO, it showed greater mass loss. Therefore, the
15 interactions of coriander EO and beta-CD in the physical mixture did not produce protection
16 and stability effects for the compounds present in the EOs.

17 Rodríguez-López et al. (2020), encapsulated linalool with hydroxypropyl beta-CD and
18 concluded that the loss of the DSC curve characteristic of this compound was indicative of the
19 formation of the IC. Sousa et al. (2022) related the Δm of the IC to the increase in the thermal
20 stability of the compounds present in the EO.

21 For the DSC of oregano EO (Figure 6A2), it was not possible to evaluate the degradation
22 peak, as the melting temperature of EO starts at around 45.3 °C, according to Fraj et al. (2019),
23 while the present test began at 50 °C. The ICs did not show endothermic peaks in the region
24 corresponding to the beta-CD dehydration process, being similar to the DSC results of coriander
25 EO. The kneading presented two consecutive endothermic events, with peaks at 301 and
26 329 °C. Co-precipitation presented two consecutive events related to the decomposition of the
27 samples. The first event peaked at 292 °C and the second event at 324 °C.

28 The TGA analysis of oregano EO (Figure 6B2) showed a Δm of 99% at 172 °C. For the
29 physical mixture, in the first endothermic event, Δm was 19%. In the interval between the
30 dehydration event and the decomposition event, Δm was 2%. The beta CD decomposition event
31 was also used as a basis, and the Δm for the physical mixture was 65%, and the total Δm was
32 92%. As the ICs did not show changes in DSC, initial Δm was evaluated at a temperature of 50
33 °C until the beginning of the endothermic degradation event. The initial Δm of kneading was
34 15%, and 69% from the beginning to the end of the beta-CD degradation process. The total Δm

1 was 91%. Co-precipitation had a Δm of 11% from 50 to 271 °C. The endothermic beta-CD
2 decomposition event generated a Δm of 76%. The % of the final mass of the complex was 6%
3 of the initial mass.

4 In this way, it was also possible to suggest the complexation of oregano EO with beta
5 CD. Kfoury et al. (2014), in their studies with different monoterpenes, observed that the
6 disappearance of the DSC peaks of the encapsulated EO compounds indicates that they did not
7 undergo dehydration or degradation.

8 For the inclusion complexes of EOs, the endothermic peaks corresponding to the water
9 volatilization process in beta-CD were not observed, nor the endothermic peak of EO
10 degradation, suggesting that the water present in the beta-CD cavity was replaced by EO, it was
11 still possible to suggest that in the physical mixture there was volatilization of the water in the
12 beta-CD cavity and the volatile compounds of the EOs that were weakly encapsulated
13 (Hădărugă et al., 2012). At TGA, the Δm of the complexes was always lower than that of a
14 beta CD at temperatures before the degradation event of this molecule. Therefore, the DSC and
15 TGA results obtained in this research corroborated those obtained in the ATR-FTIR and
16 Micro-Raman analyses, making it possible to strongly suggest the formation of ICs by both
17 methodologies, in which it is proposed that the EOs are displacing water inside the beta-CD
18 molecule, interacting with its cavity.

19

20 **3.4 Antimicrobial activity**

21 **3.4.1 Minimum Inhibitory Concentration (MIC) and Minimum Bactericidal (MBC)/ 22 Minimum Fungicide (MFC) Concentration**

23 In general, coriander EO presented higher MICs than those found for oregano EO
24 (Table 3). Satyal & Setzer (2020) related the antimicrobial and antifungal activity of coriander
25 EO with the compound linalool, with MICs varying from 97 to 16,000 µg/mL, showing that
26 coriander EO has antimicrobial activity over a wide range of concentrations. For the MIC assay,
27 an initial free EO concentration of 4000 µg/mL was used.

28

29 Table 3: MIC results of coriander and oregano EOs against the microorganisms tested.

Microorganism	MIC (µg/mL)	
	Coriander	Oregano
<i>B. subtilis</i>	>4000	500
<i>E. coli</i>	1000	250
<i>P. aeruginosa</i> ATCC15442	>4000	>4000
<i>P. aeruginosa</i> ATCC27853	4000	500
<i>S. enteritidis</i>	2000	250

<i>S. aureus</i>	>4000	500
<i>C. albicans</i>	1000	500
<i>C. parapsilosis</i>	2000	250
<i>C. tropicalis</i>	2000	500

1

2 For oregano EO, the results were promising, as the MIC varied between 250 and 500
 3 µg/mL (Table 3), especially when compared with coriander EO. The antimicrobial activity of
 4 oregano EO is due to the presence of carvacrol and thymol, which affect the cell membrane of
 5 microorganisms, altering their permeability (Khan et al., 2018; Lombrea et al., 2020). In the
 6 study by Lombrea et al. (2020), MICs for *E. coli* and *S. aureus* ranged from 0.596 to 1193
 7 µg/mL, for *P. aeruginosa* from 150 to 640 µg/mL, *S. enteritidis* from 160 µg/mL and *C.*
 8 *albicans* from 150 to 250 µg/mL. The MIC values are close to those found in the present study.
 9 It was not possible to observe the MIC for the physical mixture and ICs, due to the turbidity
 10 that beta-CD provided in the culture medium.

11 The MBC and MFC were performed based on the MIC results of free EOs. For
 12 coriander, EO, the physical mixture and ICs presented MBCs and MFCs above 4000 µg/mL.
 13 For oregano EO, the physical mixture and IC presented MBCs and CFMs higher than those
 14 found for free EO (Table 4).

15

16 Table 4: Result of MBC and CFM of oregano EO and its ICs against the tested microorganisms.

Microorganisms	CBM/CFM (µg/mL)			
	Free EO	Kneading	Co-precipitation	Physical Mixture
<i>B. subtilis</i>	500	>4000	>4000	>4000
<i>E. coli</i>	250	2000	2000	2000
<i>P. aeruginosa</i> ATCC27853	500	2000	2000	2000
<i>S. enteritidis</i>	250	2000	2000	4000
<i>S. aureus</i>	1000	2000	2000	>4000
<i>C. albicans</i>	500	1000	1000	1000
<i>C. parapsilosis</i>	500	1000	1000	1000
<i>C. tropicalis</i>	500	1000	1000	1000

17

18 The results with free oregano EO showed high antimicrobial activity. However, for the
 19 physical mixture and ICs, MBC and CFM showed a higher result than free EO, that is, the broth
 20 microdilution method was not favorable for detecting the antimicrobial activity of ICs.

21 Silva et al. (2019) investigated coriander EO in a nanospunge system containing
 22 different CDs (alpha, beta and hydroxypropyl-beta-CD) and the results demonstrated that the
 23 lowest antimicrobial activity was from the EO with beta-CD nanospunge, that is, with the
 24 oligosaccharide that has the lowest solubility and this physical property may have been a factor

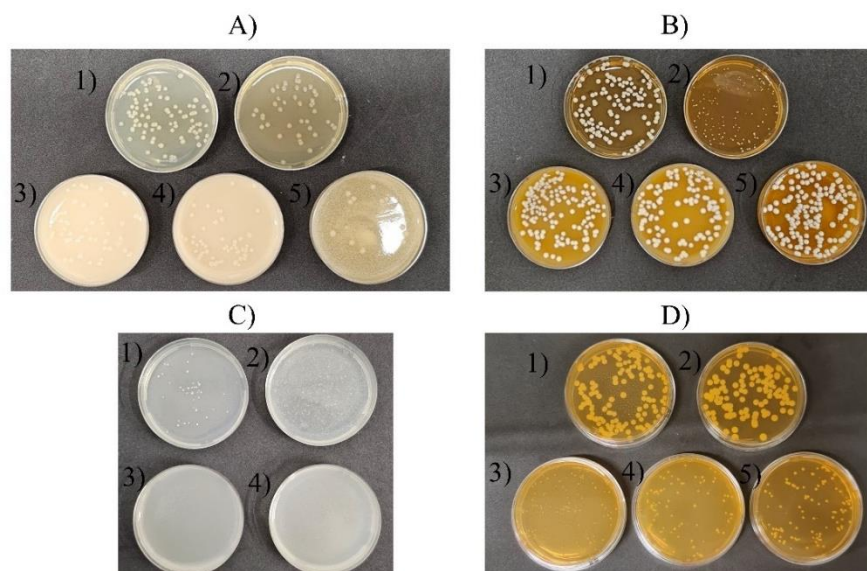
1 in interfering with the activity of the EO, in addition to the better oil release that occurred with
2 alpha-CD, as described by the authors.

3

4 **3.4.2 Agar diffusion method**

5 Coriander EO showed an inhibitory activity against the microorganisms *E. coli* and *C.*
6 *albicans* at an EO concentration of 1500 µg/mL. For the microorganism *S. aureus*, this amount
7 was higher. As for the ICs containing the equivalent of 1500 µg/mL of EO, for the bacteria *E.*
8 *coli*, it was observed that kneading and co-precipitation inhibited bacterial growth similar to
9 free EO, while the physical mixture showed a more pronounced inhibition (Figure 7A). For *C.*
10 *albicans* (Figure 7B) and *S. aureus* (undocumented), they did not show an improvement in
11 antimicrobial activity with complexation. It is worth noting that the EC% for coriander EO was
12 below 80%, resulting in a low amount of EO in the ICs, which may have affected the
13 antimicrobial activity. The low solubility of beta-CD may have been one of the factors that
14 compromised the effectiveness of the EO against microorganisms, considering that a large
15 amount of complex was required in a small amount of culture medium.

16



17
18 Figure 7: Agar diffusion method. A) Coriander EO 1500 µg/mL - *Escherichia coli*. (1) Control.
19 (2) EO. (3) Co-precipitation. (4) Kneading. (5) Physical Mixture. B) Coriander EO 1500 µg/mL
20 - *Candida albicans*. (1) Control. (2) EO. (3) Co-precipitation. (4) Kneading. (5) Physical
21 Mixture. C) Oregano EO 500 µg/mL - *Staphylococcus aureus* – after 48 h. (1) EO. (2) Physical
22 Mixture. (3) Co-precipitation. (4) Kneading. D) Oregano EO 250 µg/mL - *Candida albicans*.
23 (1) Control. (2) EO. (3) Co-precipitation. (4) Kneading. (E) Physical Mixture.

24 Oregano EO showed antimicrobial activity for the three microorganisms tested. For
25 *Staphylococcus aureus*, the inhibitory concentration was 250 µg/mL, both for free EO and ICs.

At 500 µg/mL, the free EO and the physical mixture showed inhibition of the microorganism, in which its growth was observed after 48 h, and, for the ICs, this concentration showed bactericidal activity (Figure 7C). For *Escherichia coli*, oregano EO did not show antimicrobial activity at a concentration of 500 µg/mL, however, for the ICs, this concentration was able to eliminate all microorganisms. For *Candida albicans*, at 250 and 500 µg/mL the free EO showed growth similar to the control, while for the ICs and physical mixture, at a concentration of 250 µg/mL growth inhibition was observed, and at 500 µg/mL fungicidal activity (Figure 7D). In this essay, In this test, it was possible to verify that the encapsulation process was favorable for intensifying the antimicrobial activity of oregano EO. Rodríguez-López et al. (2020) tested carvacrol and thymol encapsulated with hydroxypropyl-beta-CD and evaluated the positive effect of the complexation of these compounds, since they improve bacteriostatic activity and exert bactericidal activity.

Del Toro-Sánchez et al. (2010) claims that microbiological growth was affected by the different methodologies for detecting antimicrobial activity, a claim that explains the difference in the results obtained by the broth microdilution and agar diffusion methods.

16

17 **3.5 Antioxidant activity**

18 **3.5.1 Phenolic compounds**

Coriander EO did not present results in the analysis of total phenolics. Kačániová et al. (2020) observed the antioxidant activity of coriander EO when they used 100 µL of EO, that is, a higher concentration than in the present study.

The oregano EO presented an amount of total phenolics equivalent to 312.02 µg/mg of catechin, related to the main compound, carvacrol (Grul'ová et al., 2020; Khafaga et al., 2020). Based on these results, ABTS⁺ and DPPH free radical scavenging activities were carried out.

25

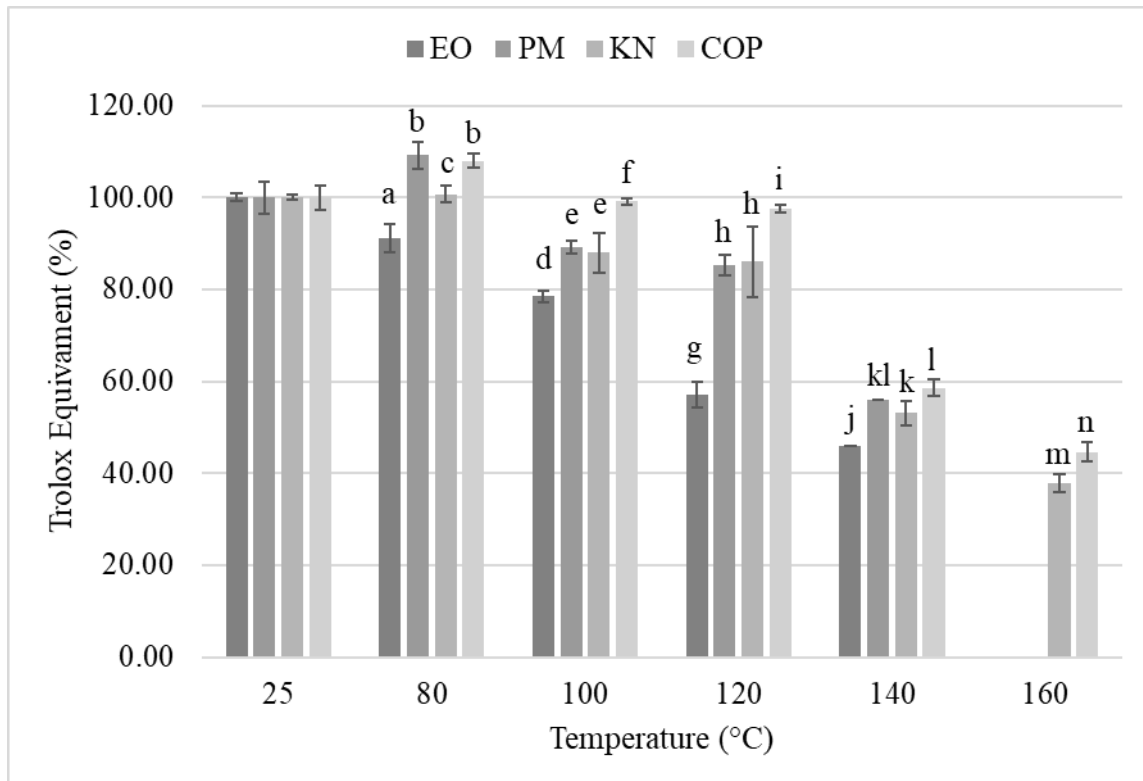
26 **3.5.2 ABTS⁺ and DPPH free radical scavenging activities and stability of antioxidant** 27 **activity at different temperatures**

Coriander EO was not evaluated in the other analyses due to the absence of phenolic compounds. Oregano EO showed low DPPH free radical scavenging activity (140 µmol Trolox/mg), therefore, the antioxidant stability test was not performed using this technique. For the ABTS⁺ free radical scavenging activity, there is an activity equivalent to 1836.33 µmol Trolox/mg.

The ABTS⁺ free radical scavenging stability for oregano EO showed that the encapsulation process was efficient (Figure 8). Kamimura et al. (2014) encapsulated the main

1 compound of oregano EO with hydroxypropyl-beta-CD and evaluated the antioxidant stability
 2 against light, but the results were not significant.

3



4
 5 Figure 8: Stability of the ABTS•+ free radical scavenging activity of (EO) Oregano, (PM)
 6 Physical Mixture, (KN) Kneading and (COP) Co-precipitation at temperatures of 25, 80, 100,
 7 120, 140 and 160 °C. ^{a, b, c, d, e, f, g, h, i, j, k, l, m, n}: The same letters do not differ significantly from
 8 each other using the Tukey test ($p \leq 0.05$).
 9

10 Considering the results obtained, the complexation of oregano EO with beta-CD
 11 promoted the protection of the EO, resulting in its stabilization against higher temperatures.
 12 Rakmai et al. (2018), evaluated the antioxidant stability of guava leaf EO and its ICs with
 13 hydroxypropyl-beta-CD against light and obtained clear results that the complexes were
 14 protected, thus reinforcing that CDs are excellent protective agents against different external
 15 factors.

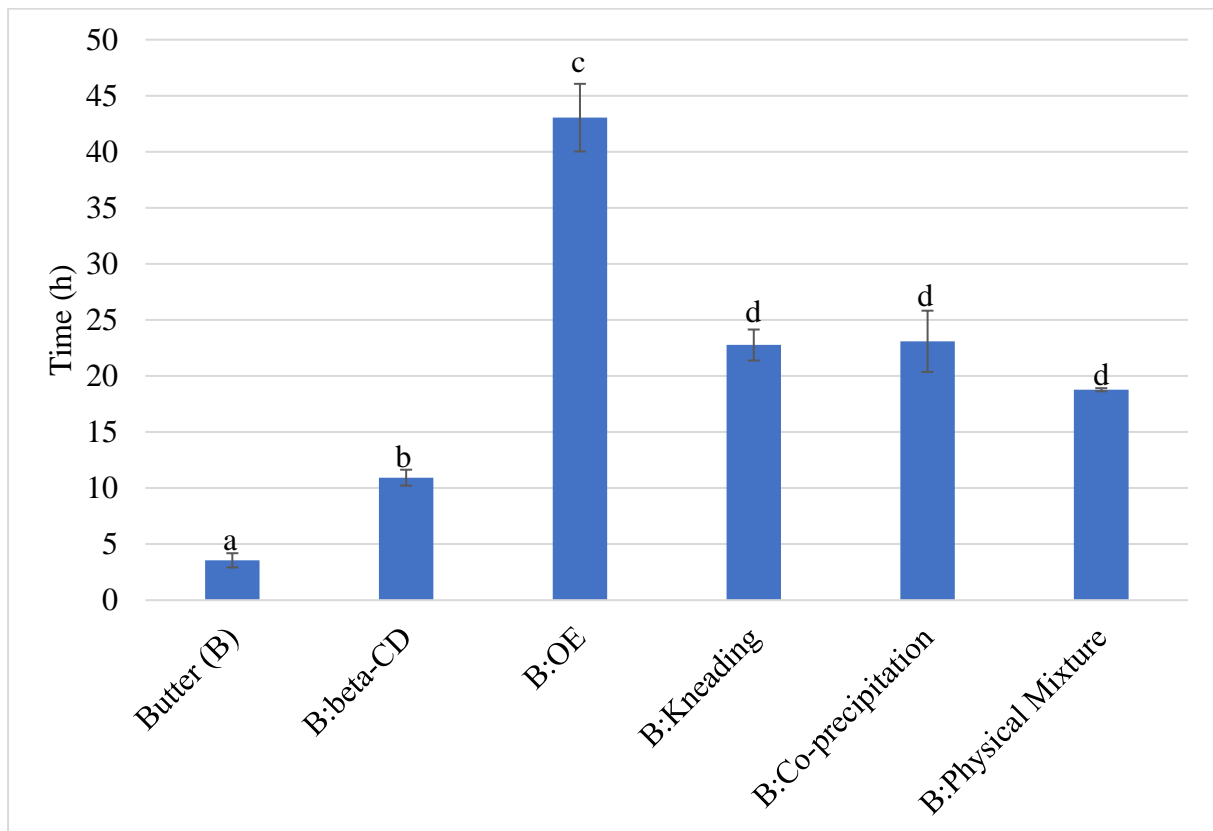
16

17 **3.6 Incorporation of EO into food and evaluation of the oxidative stability of the product**
 18 **using the Rancimat method**

19 Butter was used to incorporate oregano EO and its ICs, and the antioxidant effect on the
 20 product was evaluated using the Rancimat method at 120° C (Figure 9). The addition of ICs by
 21 kneading and co-precipitation significantly increased the oxidative stability of the butter, and

the physical mixture also presented satisfactory results, not having a significant difference in the ICs. It was also possible to verify that the addition of beta-CD itself was favorable to the oxidative stability of the butter, in which the oxidation time increased from 3.4 h to 10.6 h. When oregano EO was added to the product, it was found that the protection was even better than that observed for the ICs. This result proved to be quite interesting since it was possible to obtain an innovative, low-cost product by replacing dehydrated oregano with its EO, with good antimicrobial protection, oxidative stability and pleasant aroma.

8



9

Figure 9: Oxidative stability of butter using the Rancimat method. ^{a, b, c, d}: The same letters do not differ significantly from each other using the Tukey test ($p \leq 0.05$).

12

Pérez-López et al. (2021) complexed the compound carvacrol, present in oregano EO, with beta-CD and applied it to extra-virgin olive oil and sunflower oil, obtaining promising results for the complex, but they did not evaluate the effect of pure carvacrol on the system.

16

17 4 Conclusions

The EOs were characterized by GC-MS and the main compound of coriander EO was linalool and of oregano EO, carvacrol. The complexation efficiency (CE%) showed the best

1 results for the co-precipitation methodology in both EOs. The characterization of the ICs by
2 ATR-FTIR and Micro-Raman methodologies corroborated the DSC and TGA results and
3 allowed to strongly suggest the formation of EO-beta-CD ICs by kneading and co-precipitation
4 methodologies, due to the displacement of water from the interior of the beta-CD and
5 interaction with its cavity, while the interactions of the physical mixture with the EOs did not
6 produce protection and stability effects.

7 Antimicrobial activity was observed for both EOs, and the compounds involved in these
8 activities were linalool, thymol and carvacrol. The antimicrobial activity determination
9 methodologies used can affect the EO performance result, which was verified when
10 microdilution and agar diffusion assays were used. Coriander EO showed lower antimicrobial
11 activity when compared to oregano EO. And for ICs, bacteriostatic activity was observed for
12 coriander EO and bactericidal activity for oregano EO.

13 Oregano EO showed positive results in the determination of phenolic compounds and
14 ABTS^{•+} free radical scavenging activity. The study of antioxidant stability at high temperatures
15 indicated that beta-CD promoted protection and controlled release of EOs, making ICs an
16 alternative for products that use EOs and are exposed to varying temperatures during their
17 marketing.

18 The incorporation of oregano EO into butter and evaluation of oxidative stability using
19 the Rancimat method showed better results for pure EO, ICs and physical mixtures. Therefore,
20 this incorporation is promising in the development of low-cost and innovative products,
21 ensuring good antimicrobial protection, oxidative stability and pleasant aroma during
22 production, transport and commercialization.

23

24 Acknowledgments

25 The authors are thankful to Enzymatic Biotechnology Laboratory, Medianeira Multiuser
26 Analytical Center (CEANMED), and the Brazilian Agencies CAPES, CNPq, Finep, and
27 Fundação Araucária for their financial support of this work.

28

1 REFERENCES

- 2
- 3 Abarca, R. L., Rodríguez, F. J., Guarda, A., Galotto, M. J., & Bruna, J. E. (2016).
4 Characterization of beta-cyclodextrin inclusion complexes containing an essential oil
5 component. *Food Chemistry*, 196, 968–975. <https://doi.org/10.1016/j.foodchem.2015.10.023>
- 6 Adams, R. P. *Identification of Essential Oil Components by Gas Chromatography/Mass*
7 *Spectrometry*. (4th Edition). (2007).
- 8 Al-Shar'i, N. A., & Obaidat, R. M. (2018). Experimental and Computational Comparative
9 Study of the Supercritical Fluid Technology (SFT) and Kneading Method in Preparing β -
10 Cyclodextrin Complexes with Two Essential Oils (Linalool and Carvacrol). *AAPS*
11 *PharmSciTech*, 19(3), 1037–1047. <https://doi.org/10.1208/s12249-017-0915-x>
- 12 Castro, J. C., Pante, G. C., de Souza, D. S., Pires, T. Y., Miyoshi, J. H., Garcia, F. P.,
13 Nakamura, C. V., Mulati, A. C. N., Mossini, S. A. G., Machinski Junior, M., & Matioli, G.
14 (2022). Molecular inclusion of *Cymbopogon martinii* essential oil with β -cyclodextrin as a
15 strategy to stabilize and increase its bioactivity. *Food Hydrocolloids for Health*, 2.
16 <https://doi.org/10.1016/j.fhfh.2022.100066>
- 17 Dai, J., Hu, W., Yang, H., Li, C., Cui, H., Li, X., & Lin, L. (2022). Controlled release and
18 antibacterial properties of PEO/casein nanofibers loaded with Thymol/ β -cyclodextrin
19 inclusion complexes in beef preservation. *Food Chemistry*, 382, 132369.
20 <https://doi.org/10.1016/j.foodchem.2022.132369>
- 21 Del Toro-Sánchez, C. L., Ayala-Zavala, J. F., Machi, L., Santacruz, H., Villegas-Ochoa, M.
22 Alvarez-Parrilla, E., & González-Aguilar, G. A. (2010). Controlled release of antifungal
23 volatiles of thyme essential oil from β -cyclodextrin capsules. *Journal of Inclusion Phenomena*
24 and *Macrocyclic Chemistry*, 67(3–4), 431–441. <https://doi.org/10.1007/s10847-009-9726-3>
- 25 Fraj, A., Jaâfar, F., Martí, M., Coderch, L., & Ladhari, N. (2019). A comparative study of
26 oregano (*Origanum vulgare* L.) essential oil-based polycaprolactone nanocapsules/
27 microspheres: Preparation, physicochemical characterization, and storage stability. *Industrial*
28 *Crops and Products*, 140. <https://doi.org/10.1016/j.indcrop.2019.111669>
- 29 Gaur, S., Lopez, E. C., Ojha, A., & Andrade, J. E. (2018). Functionalization of Lipid-Based
30 Nutrient Supplement with β -Cyclodextrin Inclusions of Oregano Essential Oil. *Journal of*
31 *Food Science*, 83(6), 1748–1756. <https://doi.org/10.1111/1750-3841.14178>
- 32 Gruľová, D., Caputo, L., Elshafie, H. S., Baranová, B., de Martino, L., Sedlák, V., Gogaľová,
33 Z., Poráčová, J., Camele, I., & de Feo, V. (2020). Thymol Chemotype *Origanum vulgare* L.
34 Essential oil as a potential selective bio-based herbicide on monocot plant species. *Molecules*,
35 25(3). <https://doi.org/10.3390/molecules25030595>
- 36 Hădărugă, N. G., Hădărugă, D. I., & Isengard, H. D. (2012). Water content of natural
37 cyclodextrins and their essential oil complexes: A comparative study between Karl Fischer

- 1 titration and thermal methods. *Food Chemistry*, 132(4), 1741–1748.
2 <https://doi.org/10.1016/j.foodchem.2011.11.003>
- 3 Hanif, M. A., Nawaz, H., Naz, S., Mukhtar, R., Rashid, N., Bhatti, I. A., & Saleem, M.
4 (2017). Raman spectroscopy for the characterization of different fractions of hemp essential
5 oil extracted at 130 °C using steam distillation method. *Spectrochimica Acta - Part A: Molecular and Biomolecular Spectroscopy*, 182, 168–174.
6 <https://doi.org/10.1016/j.saa.2017.03.072>
- 7 Jentzsch, P. V., Ramos, L. A., & Ciobotă, V. (2015). Handheld Raman spectroscopy for the
8 distinction of essential oils used in the cosmetics industry. *Cosmetics*, 2(2), 162–176.
9 <https://doi.org/10.3390/cosmetics2020162>
- 10 Kačániová, M., Galovičová, L., Ivanišová, E., Vukovic, N. L., Štefániková, J., Valková, V.,
11 Borotová, P., Žiarovská, J., Terentjeva, M., Felsőciová, S., & Tvardá, E. (2020). Antioxidant,
12 Antimicrobial and Antibiofilm Activity of Coriander (*Coriandrum sativum* L.) Essential Oil
13 for Its Application in Foods. *Foods*, 9(3). <https://doi.org/10.3390/foods9030282>
- 14 Kamimura, J. A., Santos, E. H., Hill, L. E., & Gomes, C. L. (2014). Antimicrobial and
15 antioxidant activities of carvacrol microencapsulated in hydroxypropyl-beta-cyclodextrin.
16 *LWT - Food Science and Technology*, 57(2), 701–709.
17 <https://doi.org/10.1016/j.lwt.2014.02.014>
- 18 Kfouri, M., Auezova, L., Fourmentin, S., & Greige-Gerges, H. (2014). Investigation of
19 monoterpenes complexation with hydroxypropyl-β-cyclodextrin. *Journal of Inclusion Phenomena and Macrocyclic Chemistry*, 80(1–2), 51–60. <https://doi.org/10.1007/s10847-014-0385-7>
- 20 Kfouri, M., Auezova, L., Greige-Gerges, H., & Fourmentin, S. (2015). Promising
21 applications of cyclodextrins in food: Improvement of essential oils retention, controlled
22 release and antiradical activity. *Carbohydrate Polymers*, 131, 264–272.
23 <https://doi.org/10.1016/j.carbpol.2015.06.014>
- 24 Kfouri, M., Auezova, L., Greige-Gerges, H., & Fourmentin, S. (2016). Development of a
25 Total Organic Carbon method for the quantitative determination of solubility enhancement by
26 cyclodextrins: Application to essential oils. *Analytica Chimica Acta*, 918, 21–25.
<https://doi.org/10.1016/j.aca.2016.03.013>
- 27 Khafaga, A. F., Naiel, M. A. E., Dawood, M. A. O., & Abdel-Latif, H. M. R. (2020). Dietary
28 Origanum vulgare essential oil attenuates cypermethrin-induced biochemical changes,
29 oxidative stress, histopathological alterations, apoptosis, and reduces DNA damage in
30 Common carp (*Cyprinus carpio*). *Aquatic Toxicology*, 228(June), 105624.
31 <https://doi.org/10.1016/j.aquatox.2020.105624>
- 32 Khan, M., Khan, S. T., Khan, N. A., Mahmood, A., Al-Kedhairy, A. A., & Alkhathlan, H. Z.
33 (2018). The composition of the essential oil and aqueous distillate of *Origanum vulgare* L.
34 <https://doi.org/10.1016/j.aquatox.2020.105624>
- 35
- 36
- 37

- 1 growing in Saudi Arabia and evaluation of their antibacterial activity. *Arabian Journal of*
2 *Chemistry*, 11(8), 1189–1200. <https://doi.org/10.1016/j.arabjc.2018.02.008>
- 3 Li, W., Lu, B., Sheng, A., Yang, F., & Wang, Z. (2010). Spectroscopic and theoretical study
4 on inclusion complexation of beta-cyclodextrin with permethrin. *Journal of Molecular*
5 *Structure*, 981(1–3), 194–203. <https://doi.org/10.1016/j.molstruc.2010.08.008>
- 6 Liu, Y., Sameen, D. E., Ahmed, S., Wang, Y., Lu, R., Dai, J., Li, S., & Qin, W. (2022).
7 Recent advances in cyclodextrin-based films for food packaging. *Food Chemistry*,
8 370(September 2021), 131026. <https://doi.org/10.1016/j.foodchem.2021.131026>
- 9 Lombrea, A., Antal, D., Ardelean, F., Avram, S., Pavel, I. Z., Vlaia, L., Mut, A. M.,
10 Diaconeasa, Z., Dehelean, C. A., Soica, C., & Danciu, C. (2020). A recent insight regarding
11 the phytochemistry and bioactivity of *origanum vulgare* l. Essential oil. *International Journal*
12 *of Molecular Sciences*, 21(24), 1–28. <https://doi.org/10.3390/ijms21249653>
- 13 Miyoshi, J. H., Castro, J. C., Fenelon, V. C., Garcia, F. P., Nakamura, C. V., Nogueira, A. C.,
14 Ueda-Nakamura, T., de Souza, H. M., Mangolin, C. S., Moura-Costa, G. F., & Matioli, G.
15 (2022). Essential oil characterization of *Ocimum basilicum* and *Syzygium aromaticum* free
16 and complexed with β-cyclodextrin. Determination of its antioxidant, antimicrobial, and
17 antitumoral activities. *Journal of Inclusion Phenomena and Macrocyclic Chemistry*, 102(1–
18 2), 117–132. <https://doi.org/10.1007/s10847-021-01107-0>
- 19 Panda, A., Roy, P., Goon, D., Kottala, H., De, S., & Dasgupta, S. (2022). β-cyclodextrin
20 encapsulation of curcumin elicits an altered mode of angiogenin inhibition: In vitro and in
21 vivo studies. *International Journal of Biological Macromolecules*, 208(February), 654–666.
22 <https://doi.org/10.1016/j.ijbiomac.2022.03.127>
- 23 Pérez-López, A. J., Noguera-Artiaga, L., López-Miranda González, S., Gómez-San Miguel,
24 P., Ferrández, B., & Carbonell-Barrachina, Á. A. (2021). Acrylamide content in French fries
25 prepared with vegetable oils enriched with β-cyclodextrin or β-cyclodextrin-carvacrol
26 complexes. *Lwt*, 148(September 2020). <https://doi.org/10.1016/j.lwt.2021.111765>
- 27 Plati, F., Papi, R., & Paraskevopoulou, A. (2021). Characterization of oregano essential oil
28 (*Origanum vulgare* L. subsp. *hirtum*) particles produced by the novel nano spray drying
29 technique. *Foods*, 10(12). <https://doi.org/10.3390/foods10122923>
- 30 Răileanu, M., Todan, L., Voicescu, M., Ciuculescu, C., & Maganu, M. (2013). A way for
31 improving the stability of the essential oils in an environmental friendly formulation.
32 *Materials Science and Engineering: C*, 33(6), 3281–3288.
33 <https://doi.org/10.1016/j.msec.2013.04.012>
- 34 Rakmai, J., Cheirsilp, B., Mejuto, J. C., Simal-Gándara, J., & Torrado-Agrasar, A. (2018).
35 Antioxidant and antimicrobial properties of encapsulated guava leaf oil in hydroxypropyl-
36 beta-cyclodextrin. *Industrial Crops and Products*, 111(October 2017), 219–225.
37 <https://doi.org/10.1016/j.indcrop.2017.10.027>

- 1 Raveau, R., Fontaine, J., Verdin, A., Mistrulli, L., Laruelle, F., Fourmentin, S., & Sahraoui,
2 A. L. H. (2021). Chemical composition, antioxidant and anti-inflammatory activities of clary
3 sage and coriander essential oils produced on polluted and amended soils-phytomanagement
4 approach. *Molecules*, 26(17). <https://doi.org/10.3390/molecules26175321>
- 5 Rodrigues, L. B., Martins, A. O. B. P. B., Ribeiro-Filho, J., Cesário, F. R. A. S., e Castro, F.
6 F., de Albuquerque, T. R., Fernandes, M. N. M., da Silva, B. A. F., Quintans Júnior, L. J.,
7 Araújo, A. A. de S., Menezes, P. dos P., Nunes, P. S., Matos, I. G., Coutinho, H. D. M.,
8 Goncalves Wanderley, A., & de Menezes, I. R. A. (2017). Anti-inflammatory activity of the
9 essential oil obtained from Ocimum basilicum complexed with β-cyclodextrin (β-CD) in
10 mice. *Food and Chemical Toxicology*, 109, 836–846.
11 <https://doi.org/10.1016/j.fct.2017.02.027>
- 12 Rodríguez-López, M. I., Mercader-Ros, M. T., Pellicer, J. A., Gómez-López, V. M.,
13 Martínez-Romero, D., Núñez-Delicado, E., & Gabaldón, J. A. (2020). Evaluation of
14 monoterpane-cyclodextrin complexes as bacterial growth effective hurdles. *Food Control*,
15 108. <https://doi.org/10.1016/j.foodcont.2019.106814>
- 16 Satyal, P., & Setzer, W. N. (2020). Chemical Compositions of Commercial Essential Oils
17 From Coriandrum sativum Fruits and Aerial Parts. *Natural Product Communications*, 15(7).
18 <https://doi.org/10.1177/1934578X20933067>
- 19 Schulz, H., Özkan, G., Baranska, M., Krüger, H., & Özcan, M. (2005). Characterisation of
20 essential oil plants from Turkey by IR and Raman spectroscopy. *Vibrational Spectroscopy*,
21 39(2), 249–256. <https://doi.org/10.1016/j.vibspec.2005.04.009>
- 22 Shrirame, B. S., Geed, S. R., Raj, A., Prasad, S., Rai, M. K., Singh, A. K., Singh, R. S., &
23 Rai, B. N. (2018). Optimization of Supercritical Extraction of Coriander (*Coriandrum sativum*
24 L.) Seed and Characterization of Essential Ingredients. *Journal of Essential Oil-Bearing
Plants*, 21(2), 330–344. <https://doi.org/10.1080/0972060X.2018.1470943>
- 26 Siatis, N. G., Kimbaris, A. C., Pappas, C. S., Tarantilis, P. A., Daferera, D. J., & Polissiou, M.
27 G. (2005). Rapid method for simultaneous quantitative determination of four major essential
28 oil components from oregano (*Oreganum* sp.) and thyme (*Thymus* sp.) using FT-Raman
29 spectroscopy. *Journal of Agricultural and Food Chemistry*, 53(2), 202–206.
30 <https://doi.org/10.1021/jf048930f>
- 31 Silva, F., Caldera, F., Trotta, F., Nerín, C., & Domingues, F. C. (2019). Encapsulation of
32 coriander essential oil in cyclodextrin nanosplices: A new strategy to promote its use in
33 controlled-release active packaging. *Innovative Food Science and Emerging Technologies*,
34 56. <https://doi.org/10.1016/j.ifset.2019.102177>
- 35 Singleton, V. L., & Rossi, J. A. (1965). Colorimetry of Total Phenolics with
36 Phosphomolybdic-Phosphotungstic Acid Reagents. *American Journal of Enology and
37 Viticulture*, 16(3), 144–158. <https://doi.org/10.5344/ajev.1965.16.3.144>

- 1 Skoog, D. A., West, D. M., Holler, F. J., & Crouch, S. R. (2006). *Fundamentos de química*
2 analítica (Thomson, Org.; eighth ed.).
- 3 Sousa, A., Oliveira, G., Fonseca, L., Rocha, M., Rai, M., Santos, F., & de Lima, S. (2022).
4 Antioxidant Properties of Croton zehntneri Pax et Hoffm. Essential Oil and Its Inclusion
5 Complex with β -Cyclodextrin Prepared by Spray Drying. *Journal of the Brazilian Chemical*
6 *Society*. <https://doi.org/10.21577/0103-5053.20220051>
- 7 Sumalan, R. M., Alexa, E., Popescu, I., Negrea, M., Radulov, I., Obistioiu, D., & Cocan, I.
8 (2019). Exploring ecological alternatives for crop protection using coriandrum sativum
9 essential oil. *Molecules*, 24(11). <https://doi.org/10.3390/molecules24112040>
- 10 Sun, C., Cao, J., Wang, Y., Huang, L., Chen, J., Wu, J., Zhang, H., Chen, Y., & Sun, C.
11 (2022). Preparation and characterization of pectin-based edible coating agent encapsulating
12 carvacrol/HP β CD inclusion complex for inhibiting fungi. *Food Hydrocolloids*, 125, 107374.
13 <https://doi.org/10.1016/j.foodhyd.2021.107374>
- 14 Trindade, G. G. G., Thrivikraman, G., Menezes, P. P., França, C. M., Lima, B. S., Carvalho,
15 Y. M. B. G., Souza, E. P. B. S. S., Duarte, M. C., Shanmugam, S., Quintans-Júnior, L. J.,
16 Bezerra, D. P., Bertassoni, L. E., & Araújo, A. A. S. (2019). Carvacrol/ β -cyclodextrin
17 inclusion complex inhibits cell proliferation and migration of prostate cancer cells. *Food and*
18 *Chemical Toxicology*, 125, 198–209. <https://doi.org/10.1016/j.fct.2019.01.003>
- 19 Valderrama, A. C. S., & Rojas De, G. C. (2017). Traceability of Active Compounds of
20 Essential Oils in Antimicrobial Food Packaging Using a Chemometric Method by ATR-FTIR.
21 *American Journal of Analytical Chemistry*, 08(11), 726–741.
22 <https://doi.org/10.4236/ajac.2017.811053>
- 23 Vishwakarma, G. S., Gautam, N., Babu, J. N., Mittal, S., & Jaitak, V. (2016). Polymeric
24 Encapsulates of Essential Oils and Their Constituents: A Review of Preparation Techniques,
25 Characterization, and Sustainable Release Mechanisms. *Polymer Reviews*, 56(4), 668–701.
26 <https://doi.org/10.1080/15583724.2015.1123725>